

2009

# Combustion and emissions characteristics of a compression-ignition engine using dual ammonia-diesel fuel

Aaron Reiter  
*Iowa State University*

Follow this and additional works at: <http://lib.dr.iastate.edu/etd>



Part of the [Mechanical Engineering Commons](#)

---

## Recommended Citation

Reiter, Aaron, "Combustion and emissions characteristics of a compression-ignition engine using dual ammonia-diesel fuel" (2009).  
*Graduate Theses and Dissertations*. 10560.  
<http://lib.dr.iastate.edu/etd/10560>

This Thesis is brought to you for free and open access by the Graduate College at Iowa State University Digital Repository. It has been accepted for inclusion in Graduate Theses and Dissertations by an authorized administrator of Iowa State University Digital Repository. For more information, please contact [digirep@iastate.edu](mailto:digirep@iastate.edu).

**Combustion and emissions characteristics of a compression-ignition engine using dual  
ammonia-diesel fuel**

by

Aaron Jesse Reiter

A thesis submitted to the graduate faculty  
in partial fulfillment of the requirements for the degree of  
MASTER OF SCIENCE

Major: Mechanical Engineering

Program of Study Committee:  
Song-Charng Kong, Major Professor  
Balaji Narasimhan  
Gap-Yong Kim

Iowa State University

Ames, Iowa

2009

Copyright © Aaron Jesse Reiter, 2009. All rights reserved.

## Table of Contents

<b>Table of Contents .....</b>	<b>ii</b>
<b>List of Figures.....</b>	<b>iv</b>
<b>List of Tables.....</b>	<b>vii</b>
<b>Acknowledgements.....</b>	<b>viii</b>
<b>Abstract.....</b>	<b>ix</b>
<b>Chapter 1 Introduction.....</b>	<b>1</b>
<b>1.1 Motivation .....</b>	<b>1</b>
<b>1.2 Objective .....</b>	<b>3</b>
<b>Chapter 2 Literature Review .....</b>	<b>5</b>
<b>2.1 Introduction .....</b>	<b>5</b>
<b>2.2 Usage of Ammonia .....</b>	<b>5</b>
<b>2.3 Ammonia as a Fuel.....</b>	<b>7</b>
2.3.1 Ammonia Feasibility as a Fuel .....	8
2.3.2 Experimental Results as a Fuel.....	11
2.3.2.1 Ammonia as a Spark-Ignition Engine Fuel .....	12
2.3.2.2 Ammonia as a Compression-Ignition Engine Fuel.....	14
2.3.2.3 Ammonia as a Fuel in a Compression Ignition and Spark Ignition Application.....	18
2.3.2.4 Comparing the Army Papers .....	21
<b>2.4 Ammonia as a Diesel Exhaust NO<sub>x</sub> Reducing Agent.....</b>	<b>22</b>
2.4.1 Selective Catalytic Reduction (SCR).....	22
2.4.2 Selective Non-Catalytic Removal (SNCR).....	24
2.4.3 Discussion on Post Combustion NO <sub>x</sub> Removal .....	27
2.4.4 Diesel NO <sub>x</sub> Reduction In-Cylinder .....	28
<b>2.5 Summary .....</b>	<b>29</b>
<b>Chapter 3 Methods and Procedures.....</b>	<b>32</b>
<b>3.1 Engine System Design .....</b>	<b>32</b>
3.1.1 Engine Specifications .....	32
3.1.2 Fuel System .....	33
3.1.1.1 Ammonia Flow Control System.....	35
<b>3.2 Engine Testing Methods .....</b>	<b>38</b>
3.2.1 Constant Peak Torque Testing .....	39
3.2.2 Minimum Diesel Fueling with Variable Ammonia Flow Rates .....	39
3.2.3 Test Fuels.....	40
<b>3.3 Engine Parameter Measurement and Analysis .....</b>	<b>40</b>
3.3.1 Ammonia Concentration Measurement .....	40
3.3.1.1 Ammonia Concentration Measurement Equipment .....	41
3.3.1.2 Ammonia Concentration Measurement Procedure.....	44

3.3.2 Gaseous Emission Analysis .....	46
3.3.3 Exhaust Emissions and Engine Efficiency Analysis.....	48
3.3.4 Exhaust Particulate Matter Analysis.....	55
3.3.5 Brake Specific Fuel Consumption Analysis .....	55
3.2.5 Cylinder Pressure Measurement .....	56
<b>Chapter 4 Results .....</b>	<b>57</b>
<b>4.1 Baseline Testing with Diesel Fuel.....</b>	<b>57</b>
<b>4.2 Testing with Ammonia and Diesel Fuel .....</b>	<b>62</b>
4.2.1 Constant Peak Torque Testing with Ammonia .....	63
4.2.3 Minimum Diesel Fueling with Variable Ammonia Flow Rates .....	77
4.2.4 Engine Tests Using Biodiesel .....	84
4.2.5 Oil Analysis .....	89
<b>Chapter 5 Summary and Discussion .....</b>	<b>90</b>
<b>5.1 Conclusions .....</b>	<b>90</b>
<b>5.2 Future Study Recommendations .....</b>	<b>91</b>
<b>Bibliography .....</b>	<b>93</b>

## List of Figures

Figure 3.1 – JD 4045 Stanadyne DB4 rotary injection pump timing map.....	34
Figure 3.2 – Ammonia intake location.....	35
Figure 3.3 – Ammonia storage tanks. ....	36
Figure 3.4 – Ammonia fueling system. ....	37
Figure 3.5 – Orifice plate flow restrictor.....	38
Figure 3.6 – Ammonia concentration sampling probe location. ....	41
Figure 3.7 – Sampling probe. ....	42
Figure 3.8 – Ammonia concentration sampling train.....	43
Figure 4.1 - Torque vs. load curves for diesel only operation. ....	57
Figure 4.2 – Power vs. load curve for diesel only operation.....	58
Figure 4.3 – BSFC vs. load curves for diesel only operation.....	58
Figure 4.4 – CO emissions under diesel only operation. ....	59
Figure 4.5 – CO <sub>2</sub> emissions under diesel only operation. ....	60
Figure 4.6 – HC emissions under diesel only operation. ....	60
Figure 4.7 – NO emissions under diesel only operation. ....	61
Figure 4.8 – Soot emissions under diesel only operation.....	61
Figure 4.9 – Engine torque and energy replacement data while operating on ammonia and diesel fuel at 1400 rpm. ....	62
Figure 4.10 – Engine torque and energy replacement data while operating on ammonia and diesel fuel at 1800 rpm. ....	63
Figure 4.11 – Measured power output of engine under constant peak torque operation at 1000 rpm. ....	65
Figure 4.12 – Measured torque output of engine under constant peak torque operation at 1000 rpm. ....	65
Figure 4.13 – Measured engine BSFC data under constant peak torque operation at 1000 rpm. ....	66
Figure 4.14 – Measured fuel flow under constant peak torque operation at 1000 rpm. ....	66
Figure 4.15 - Exhaust NO emissions under constant peak torque operation at 1000 rpm. ....	67

Figure 4.16 – Exhaust CO emissions under constant peak torque operation at 1000 rpm. ....	68
Figure 4.17 – Exhaust HC emissions under constant peak torque operation at 1000 rpm. ....	68
Figure 4.18 – Exhaust soot emissions under constant peak torque operation at 1000 rpm. ....	69
Figure 4.19 – Exhaust CO <sub>2</sub> emissions under constant peak torque operation at 1000 rpm. ....	69
Figure 4.20 – Exhaust ammonia concentration, ppmV, under constant peak torque operation at 1000 rpm. ....	71
Figure 4.21 – Exhaust ammonia concentration, g/kW-hr, while under constant peak torque operation at 1000 rpm. ....	72
Figure 4.22 – Intake vs. exhaust mass flow of ammonia under constant peak torque operation at 1000 rpm. ....	74
Figure 4.23 – Combustion efficiency of ammonia under constant peak torque operation at 1000 rpm. ....	74
Figure 4.24 – In-cylinder pressure history and heat release rate for 100% diesel fuel and combined diesel-ammonia (20% diesel plus 80% NH <sub>3</sub> ) under constant peak torque operation. ....	75
Figure 4.25 – In-cylinder pressure history and heat release rate for 100% diesel fuel and combined diesel-ammonia (40% diesel plus 60% NH <sub>3</sub> ) under constant peak torque operation. ....	76
Figure 4.26 – In-cylinder pressure history and heat release rate for 100% diesel fuel and combined diesel-ammonia (60% diesel plus 40% NH <sub>3</sub> ) under constant peak torque operation. ....	76
Figure 4.27 – In-cylinder pressure history and heat release rate for 100% diesel fuel and combined diesel-ammonia (80% diesel plus 20% NH <sub>3</sub> ) under constant peak torque operation. ....	77
Figure 4.28 – Measured engine power under variable ammonia flow rate operation at 1000 rpm. ....	79
Figure 4.29 – Measured engine torque under variable ammonia flow rate operation at 1000 rpm. ....	79
Figure 4.30 – Measured fuel flow rate data under variable ammonia flow rate operation at 1000 rpm. ....	80
Figure 4.31 – Measured BSFC data under variable ammonia flow rate operation at 1000 rpm. ....	80

Figure 4.32 – Ammonia concentration in the exhaust, ppmV, under 5% diesel energy with ammonia flow rate operation at 1000 rpm.....	81
Figure 4.33 – Ammonia concentration in the exhaust, g/kW-hr, under 5% diesel energy with variable ammonia flow rate operation at 1000 rpm. ....	81
Figure 4.34 – Combustion efficiency of ammonia under 5% diesel energy with variable ammonia flow rate operation at 1000 rpm. ....	82
Figure 4.35 – Cylinder pressure histories and heat release rate data for 20% engine load using two different operations at 1000rpm.....	83
Figure 4.36 – Cylinder pressure histories and heat release rate data for 60% engine load using two different operations at 1000rpm.....	84
Figure 4.37 – Measured engine torque under constant peak torque operation at 1000 rpm using NH <sub>3</sub> and B100.....	85
Figure 4.38– Measured BSFC under constant peak torque operation at 1000 rpm using NH <sub>3</sub> and B100.....	85
Figure 4.39 – Measured engine torque under variable ammonia flow rate operation at 1400 rpm using NH <sub>3</sub> and B100.....	86
Figure 4.40 – Measured BSFC under variable ammonia flow rate operation at 1400 rpm using NH <sub>3</sub> and B100.....	86
Figure 4.41 – Measured HC and NO <sub>x</sub> emissions of B100 only.....	87
Figure 4.42 – Measured CO <sub>2</sub> emissions of B100 only.....	87
Figure 4.43 – Measured NO <sub>x</sub> emissions of B100 and ammonia under constant peak torque operation.....	88
Figure 4.44 – Measured HC emissions of B100 and ammonia under constant peak torque operation.....	88
Figure 4.45 – Measured CO <sub>2</sub> emissions of B100 and ammonia under constant peak torque operation.....	89

## List of Tables

Table 2.1 – Properties of various internal combustion fuels (National Institute of Standards and Technology, 2009) .....	9
Table 2.2 – Combustion properties of various internal combustion fuels (Saika, et al., 2006) .....	10
Table 2.3 – Cost comparison of transportation systems used when each fuel is used in a hydrogen combustion turbine which generates a power output of 1000MW (Sato, et al., 1998). .....	11
Table 3.1 – Engine Specifications.....	33
Table 4.1 – Health symptoms due to ammonia exposure (United States Occupational Safety and Health Administration, 2009). .....	73
Table 4.2 – Oil sample data as tested by U.S. Oil.....	89

## **Acknowledgements**

I especially want to thank Dr. Song-Charng Kong for being my major professor and allowing me to participate in this interesting study. He has provided me with much insight and guidance in my quest for knowledge.

I would like to acknowledge Iowa Energy Center for financial support in order to conduct this study. Helpful comments by Mr. Norman Olson are very much appreciated. I also want to thank Dr. Balaji Narasimhan and Dr. Gap-Yong Kim for being on my committee.

I want to thank Matthias Veltman, Anthony Phan, Prashanth Karra, Najeeb Kuzhiyil, Zach McVey, Nathan Gibilisko, and Lukas Shea for providing help when I needed it. They are true friends, and someday, I hope I can help them as much as they helped me.

I want to thank Jim Dautremont and Larry Couture for providing their wealth of experience and knowledge even when I asked too many questions. I also would like to thank Allison Mickelson for putting up with me and being patient with paper work.

Finally I would like to thank my family and Stacie for being patient, providing support, and keeping my nose to the grindstone. Without their love and support I don't know where I would be.

## **Abstract**

This study investigated the performance of a compression-ignition engine using a dual-fuel approach with ammonia and diesel fuel. With the world's increasing need for alternative energy and clean emissions, ammonia stands out as a viable candidate since its combustion does not produce the known greenhouse gas, carbon dioxide. Ammonia is one of the world's most synthesized chemicals and its infrastructure is well established. Ammonia can be regarded as a hydrogen carrier and used as a fuel. However, ammonia is highly resistant to autoignition and readily vaporizes under atmospheric conditions. Therefore, this study introduced ammonia vapor into the engine intake manifold and used the existing diesel injection system to inject diesel fuel or biodiesel to initiate combustion in the cylinder. The test engine was a four-cylinder, turbocharged diesel engine with slight modifications to the intake manifold for ammonia induction.

An ammonia fueling system was developed in order to control and measure the amount of ammonia allowed into the engine. Dynamometer tests were performed to measure the engine power, fuel consumption, in-cylinder pressure histories, and exhaust emissions.

Engine test results showed that ammonia could be burned in a compression-ignition engine using the present dual-fuel approach. Various combinations of amounts of ammonia and diesel fuel were successfully tested using two major engine operation schemes. One scheme was to use different combinations of ammonia and diesel fuel to achieve a constant peak torque equal to that of 100% diesel only combustion. And the other was to use a

minimum quantity of diesel fuel and vary the amount of ammonia to achieve variable engine loads.

Under constant peak torque operation, in order to achieve favorable fuel efficiency, the preferred operation range was to use 40 ~ 60% energy provided by diesel fuel in conjunction with 60 ~ 40% energy supplied by ammonia. Exhaust carbon monoxide and hydrocarbon emissions using the dual-fuel approach were generally higher than that of using pure diesel fuel, while nitrogen oxides (NO<sub>x</sub>) emissions varied with different fueling combinations. NO<sub>x</sub> emissions could be reduced using the dual-fuel operation if ammonia accounted for less than 40% of the total fuel energy due to the lower combustion temperature resulting in lower thermal NO<sub>x</sub>. If ammonia accounted for the majority of the fuel energy, NO<sub>x</sub> emissions increased significantly due to fuel-bound nitrogen. On the other hand, soot emissions could be reduced significantly if a significant amount of ammonia was used due to the lack of carbon present in the combination of fuels. Despite the overall high ammonia conversion efficiency (nearly 100%), exhaust ammonia emissions ranged from 1,000 to 3,000 ppmV and further after-treatment will be required due to health concerns.

The variable engine load operation resulted in relatively poor fuel efficiency due to the lack of diesel energy to initiate effective combustion. Exhaust ammonia emissions ranged between 4,000 and 12,000 ppmV under the conditions studied.

In-cylinder pressure history was analyzed to obtain the heat release rate data and combustion phasing. Results indicated that ignition delay increased with increasing amounts of ammonia due to its high resistance to autoignition. As a result, the peak cylinder pressure decreased because of the lower combustion temperature of ammonia. Engine testing using

combinations of ammonia and biodiesel (B100) were also performed and results had the same trends as using the ammonia-diesel approach. It is recommended that further combustion optimization using direct liquid ammonia injection be performed to increase combustion efficiency and reduce exhaust ammonia emissions.

## Chapter 1 Introduction

### 1.1 Motivation

Nowadays, the focus for the world to become independent of carbon-based fuels is becoming increasingly important. The world as a whole in 2007 consumed roughly 85.22 billion barrels of oil per day (Central Intelligence Agency, 2009). In July 2008 oil traded as high as \$145/barrel on the New York Stock Exchange (Williams, 2009). With oil supplies dwindling this has caused the public to drastically rethink its usage habits and energy sources.

In conjunction with the need to rid our dependence on fossil fuels, climate change has also become increasingly important to the public. According to many sources, and varying thought groups within the scientific community, human activity has caused the most rapid climate change the planet has ever seen. Transportation sources, energy production, and industrial processes all emit harmful green house gases. Of critical importance is the need to develop new sources of energy that are non-polluting, renewable, safe, available at reasonable costs, and in amounts sufficient enough to meet the world's energy needs.

As early as World War II, people tried using ammonia as an alternative to fossil based fuels being consumed by the war effort (Koch, 1945). This led the U.S. Army to fund a series of experimental works to test the feasibility using ammonia as an alternative fuel source in the 1960's (Gray, et al., 1966; Pearsall and Garabedian, 1967; Starkman, et al., 1966). However, until the 1990's, not much work had been done on the subject, due to the low cost of petroleum based fuels (Broadmeadow and Ibrahim, 1995; Miyamoto, et al., 1995).

Besides being carbon-free ammonia has several desirable attributes. It has a high energy density, it is relatively easy to store as a liquid or a gas, and it is one of the world's most synthesized chemicals (ICIS, 2007). However, its ignition temperature is relatively high at 650 °C, and it must be combusted in concentrations of 16-25% by volume in air.

In the U.S. Army studies, it was shown that ammonia could provide sustainable combustion when used as a primary fuel or in conjunction with a pilot fuel or spark source in either spark-ignition (SI) and compression-ignition (CI) combustion schemes. However, each method had its own advantages and drawbacks.

In order to combust ammonia in a CI engine the compression ratio (CR) must be very high (approximately 30:1), or there must be a pilot ignition source available to provide sufficient ignition energy. It was shown that spark ignition applications could produce sustainable combustion with ammonia as a primary fuel but only approximately 70% output could be achieved. Experiments with both gaseous and liquid injection were attempted but gaseous injection proved to be the most effective and provide the most stable combustion.

Ammonia also has the potential to be an effective nitrogen oxide reducing agent in which several methods have been developed and proven successful. Nitrogen oxides (NO<sub>x</sub>) are formed when fuels are burned at high temperatures in applications such as transportation vehicles and stationary combustion sources including electric utility and industrial boilers. NO<sub>x</sub> compounds play an important role in atmospheric reactions that create harmful particulate matter, ground-level ozone, smog, and acid rain (Environmental Defense Fund, 2002).

National emissions of NO<sub>x</sub> have actually increased over the past 30 years by about 19%, whereas all the other major criteria air pollutants (carbon monoxide, lead, ozone, particulate matter and sulfur dioxide) have decreased since the advent of the modern Clean Air Act in 1970 (Environmental Defense Fund, 2002).

The first attempts at using ammonia as a NO<sub>x</sub> reduction agent were in the power generation industries in the 1980's (Kimball-Linne and Hanson, 1986) and recently research has migrated to the automotive industry, specifically in diesel fueled CI engines (Caton and Xia, 2004; Miyamoto, et al., 1995). Retarded fuel injection timings, exhaust gas recirculation (EGR), and water injection have long been common methods for reducing NO<sub>x</sub> in diesel exhaust. All of these methods have the same desired effect, in which they lower the combustion temperature or oxygen concentration of the in-cylinder mixture. However, a larger NO<sub>x</sub> reduction without interference to combustion efficiency has not been achieved. Catalytic after-treatment methods to deoxidize NO<sub>x</sub> using urea and various catalytic surfaces have also been investigated, but these methods suffer by having short durability from plugging due to soot, and a narrow temperature range in which they are effective. Some success has been shown, but new NO<sub>x</sub> reduction techniques are needed to meet increasingly stringent upcoming federal emissions standards.

## **1.2 Objective**

This project's focus is to study the combustion and emissions characteristics of a compression-ignition engine that burns ammonia and pilot diesel fuel with minimum modification. The engine is a multi-cylinder, turbocharged diesel engine manufactured by

John Deere (Model 4045) and is used in various tractor applications. Since ammonia vaporizes at ambient pressures lower than 5 bar and has a very high resistance to autoignition, we propose to introduce ammonia gas directly into the engine intake manifold to form a premixed mixture in the cylinder and use the original fuel injection system to inject diesel fuel or biodiesel as a pilot fuel to ignite the mixture. Ammonia will be injected in a location after the turbocharger compressor into the intake pipe. A flow system will be developed to control and measure the amount of ammonia allowed into the engine.

Dynamometer tests will be performed to measure the engine power, fuel consumption and exhaust emissions. Appropriate operating ranges will be identified using various combinations of ammonia and pilot diesel fuel. Ratios of energy substitution by ammonia for stable combustion without sacrificing engine performance will be investigated. Exhaust emissions as a function of ammonia-diesel fuel ratios will be measured including soot, nitrogen oxides, carbon monoxides, carbon dioxides and unburned hydrocarbons.

## Chapter 2 Literature Review

### 2.1 Introduction

Ammonia is the basic building block of the world's nitrogen industry and is the intermediate product from which a wide variety of nitrogen-based fertilizers and industrial products are produced. Fertilizer use alone accounts for 85% of the world's ammonia demand (ICIS, 2007) and 1% of all man-made power is used for its synthesis (Ullmann's Encyclopedia of Industrial Chemistry, 2006).

### 2.2 Usage of Ammonia

Although ammonia is a common byproduct of decomposition, the most common method for commercially producing ammonia is the Haber-Bosch process. This involves combining elemental nitrogen with hydrogen. Most often the hydrogen used for synthesis is sourced from decomposed methane found in natural gas. In order for the gases to combine chemically they need to be heated to 500°C, pressurized to approximately 150-200atm and passed over an iron catalyst (Modak, 2002). The exothermic reaction is as follows:



$$\Delta H_{298K} = -45.7 \frac{kJ}{mol} \quad (2.2)$$

Ammonia synthesis can be split into two processes: a hydrogen and nitrogen production process and an ammonia synthesis process. The hydrogen may be produced by natural gas reforming (steam or autothermal), coal gasification, water electrolysis, or steam-

iron reaction (Saika, et al., 2006). Production of hydrogen is the major contributor to of energy consumption during ammonia synthesis. However, ammonia produced from water electrolysis is more expensive than ammonia produced from natural gas (Saika, et al., 2006).

Ammonia-based fertilizers are usually a form of processed ammonia and include urea ( $\text{CH}_4\text{N}_2\text{O}$ ), ammonium nitrates (basic form,  $\text{H}_4\text{N}_2\text{O}_3$ ), ammonium sulphate ( $\text{H}_8\text{N}_2\text{O}_4\text{S}$ ), and ammonium phosphates. Ammonia cannot be applied directly to the ground as a fertilizer, it must first be converted to ammonium ( $\text{NH}_4^+$ ) and nitrates in order to be absorbed by plants (ICIS, 2007).

Other common uses of ammonia are as a refrigerant and a cleaning and bleaching agent for household cleaner. Ammonia is a versatile chemical and is also used for the production of hexamethylenediamine for nylon, acrylonitrile for fibers and plastics, caprolactum for nylon, isocyanates for polyurethanes and hydrazine (ICIS, 2007). It is a catalyst in phenol-formaldehyde condensation and present in urea-formaldehyde condensation used to make synthetic resins (ICIS, 2007). Ammonium nitrate is used as the main ingredient in explosives, while its medical grade component is decomposed into nitrous oxide (ICIS, 2007).

Urea is a more stable and safe chemical similar to ammonia. It is commercially available and is both ground-water compatible and chemically stable under ambient conditions (Alkemade and Schumann, 2006). Urea plants are often integrated into ammonia production plants since the urea synthesis process requires the carbon dioxide by-product produced from ammonia production (ICIS, 2007). Urea is the fastest growing nitrogen product and is mainly used in North America and Europe as a fertilizer (ICIS, 2007).

However, in recent years, urea has become the primary focus as a reducing agent used in NOx Selective Catalytic Reduction (SCR), which will be discussed later in this chapter.

In 2006, ammonia production was 148 million tonnes worldwide, which was a 2% increase from 2005 production (ICIS, 2007). The most significant increases were in China, the Middle East, and Australia while production declined in the U.S. and Europe. The rising trend and volatility in energy prices, especially natural gas, has impacted the economics of ammonia production in key producing and consuming countries. Countries or regions with a large consumption base and a reliance on imports of natural gas registered a steep decline in ammonia capacity (ICIS, 2007). Countries benefiting from low cost feedstock prices have expanded ammonia capacity, dedicated for export.

Ammonia, like every other commodity, has a direct correlation to the world's economic lifeline. At times of record crude prices, in September of 2008, ammonia peaked at \$930 per tonne. While in November of the same year contract prices plummeted to \$575 per tonne (Hui, et al., 2008). The lowest cost ammonia source is coal with a production cost of \$147-\$432 per ton, which results in a gasoline equivalent cost of \$0.96-\$2.83 per gallon (Bartels, 2008). Natural gas and ocean thermal energy conversion (OTEC) both provide a cost of \$689 per ton, which results in a gasoline equivalent of \$4.51 per gallon (Bartels, 2008).

## **2.3 Ammonia as a Fuel**

As early as World War II, people tried using ammonia as an alternative to fossil based fuels being consumed by the war effort (Koch, 1945). This led the U.S. Army to fund a series

of experimental works to test the feasibility using ammonia as an alternative fuel source in the 1960's (Gray, et al., 1966; Pearsall and Garabedian, 1967; Starkman, et al., 1966). However, until the 1990's, not much work had been done on the subject, due to the low cost of petroleum based fuels (Broadmeadow and Ibrahim, 1995; Miyamoto, et al., 1995).

### **2.3.1 Ammonia Feasibility as a Fuel**

Besides being a carbon-free fuel, ammonia has many desirable characteristics. It can be easily liquefied for storage at a relatively low pressure (150 psi) at ambient temperature (similar to liquid propane) or cooled to  $-33^{\circ}\text{C}$  to be stored at ambient pressures. It has a high octane rating of 110 (i.e. highly resistant to autoignition). It contains 17.8 wt% of hydrogen and stores 30% more energy by volume than liquid hydrogen (MacKenzie and Avery, 1996). It is also more easily dissociated using 16% of the energy in the fuel and requires no energy for the final hydrogen purification stage (Saika, et al., 2006). Ammonia has relatively the same properties as liquid propane ( $\text{C}_3\text{H}_8$ ) but has a relatively high ignition temperature of  $650^{\circ}\text{C}$ . Ammonia and propane have nearly the same densities, boiling points ( $-33.3^{\circ}\text{C}$  for ammonia,  $-42.0^{\circ}\text{C}$  for propane), and octane numbers (National Institute of Standards and Technology, 2009) as can be seen in Table 2.1. Propane is already a widely used transportation fuel with roughly 270,000 vehicles already on the road (Energy Information Administration, 1998). In fact, the same infrastructure could be used to transport and store ammonia as long as all brass, copper, and rubber based materials are replaced with mild steel and Teflon counterparts.

**Table 2.1 – Properties of various internal combustion fuels (National Institute of Standards and Technology, 2009)**

<b>Fuel</b>	<b>Liquid H<sub>2</sub></b>	<b>Gaseous H<sub>2</sub></b>	<b>Natural Gas</b>	<b>Ammonia</b>	<b>Propane</b>	<b>Gasoline</b>	<b>Methanol</b>
<b>Formula</b>	H <sub>2</sub>	H <sub>2</sub>	CH <sub>4</sub>	NH <sub>3</sub>	C <sub>3</sub> H <sub>8</sub>	C <sub>8</sub> H <sub>18</sub>	CH <sub>3</sub> OH
<b>Storage Method</b>	Cryogenic Liquid	Compressed Gas	Compressed Gas	Liquid	Liquid	Liquid	Liquid
<b>Approximate AKI<sup>*</sup> Octane Rating</b>	RON >130 MON very low	RON >130 MON very low	107	110	103	87-93	113
<b>Storage Temp [°C]</b>	-253	25	25	25	25	25	25
<b>Storage Pressure [kPa]</b>	102	24,821	24,821	1030	1020	101.3	101.3
<b>Fuel Density [kg/m<sup>3</sup>]</b>	71.1	17.5	187.2	602.8	492.6	698.3	786.3
<b>Heat Storage</b>							
LHV [MJ/kg]	120.1	120.1	38.1	18.8	45.8	42.5	19.7
[MJ/L]	8.5	2.1	7.1	11.3	22.6	29.7	15.5
<b>Fuel Requirement to Match Energy of 10 Gallons of Gasoline [MJ]</b>	1123.3	1123.3	1123.3	1123.3	1123.3	1123.3	1123.3
<b>Fuel Volume [L]</b>	131.5	534.4	157.5	99.2	49.8	37.9	72.5
<b>Fuel Weight [kg]</b>	9.4	9.4	29.5	59.8	24.5	26.4	57.0

\*Anti-Knock Index, (RON+MON)/2

Ammonia has safer handling properties when compared to hydrogen. Hydrogen can produce an easy flashback with its high burning velocity and low minimum ignition energy as seen in Table 2.2. Hydrogen must also be stored at relatively high pressures at ambient temperatures (2500-10,000 psi), or stored as liquid when chilled to -250°C (MacKenzie and Avery, 1996). Both of these storage systems are more costly than tanks needed to store ammonia because of the need for heavier construction or lower storage temperatures.

Ammonia storage systems are also more efficient at 93.6% when including synthesis energy in calculation as compared to hydrogen storage systems at 76.9% (Bartels, 2008).

**Table 2.2 – Combustion properties of various internal combustion fuels (Saika, et al., 2006)**

<b>Combustion Property</b>	<b>NH<sub>3</sub></b>	<b>H<sub>2</sub></b>	<b>C<sub>8</sub>H<sub>18</sub> (Octane)</b>	<b>CH<sub>3</sub>OH (methanol)</b>
Net heat of combustion (MJ/kg)	18.8	120.0	44.6	19.2
Flammability limits (% by volume in air)	15-28	4.7-75	1-6.5	6.7-36
Laminar burning velocity (m/s)	0.015	3.51	0.58	0.71
Spontaneous ignition temperature (°C)	651	571	230	470
Minimum ignition energy (mJ)	8.0	0.018	0.28	0.14

In terms of energy, world ammonia production (recently about 150 million tons per year) is equivalent to about 1.3 million barrels per day of gasoline (MacKenzie and Avery, 1996). For comparison, the U.S. gasoline consumption is about 7.5 million barrels per day (MacKenzie and Avery, 1996). In terms of cost, ammonia is \$200-300 per ton while crude oil is \$160-230 per ton. Therefore, both fuels have very similar costs by weight. When comparing the cost of transportation systems in 1998, ammonia and hydrogen were approximately 33 yen/kWh, almost equivalent to that of methanol (24.70 yen/kWh) (Sato, et al., 1998), as can be seen in Table 2.3.

**Table 2.3 – Cost comparison of transportation systems used when each fuel is used in a hydrogen combustion turbine which generates a power output of 1000MW (Sato, et al., 1998).**

<b>Case</b>	<b>Liquid Hydrogen</b>	<b>Methanol</b>	<b>Ammonia</b>
Raw fuel generation cost on arrival basis (yen/MJ)	2.52	1.43	1.66
Hydrogen fuel generation cost (yen/MJ)	3.85	2.39	3.75
Power generation cost (yen/kW-hp) (transmission end power amount basis)	32.64	24.70 (30.83)*	32.93

\*Parenthesized is the power generation cost including CO<sub>2</sub> recovery and processing

Ammonia is also an attractive element in a hydrogen based fuel cell. In an alkaline fuel cell, ammonia can be converted to a mixture of hydrogen and nitrogen by recycling heat generated by the fuel cell (MacKenzie and Avery, 1996). Fuel cells convert chemical energy directly into electrical energy and can attain efficiencies of 60% or higher (MacKenzie and Avery, 1996). In a motor vehicle-based application, the fuel cell could be used indirectly to propel the vehicle. The fuel cell would create electricity which could be used to power direct drive electric motors.

### **2.3.2 Experimental Results as a Fuel**

Logistics studies of U.S. Army operation in WWII and the Korean War established that approximately 65% of the total tonnage required for support of combat operations consisted of fuels and lubricants (Pearsall and Garabedian, 1967). This led the U.S. military to explore experimentation with alternative fuels and to initiate a project in which ammonia

was examined as a fuel for internal combustion engines. Various research groups were funded by this project and produced technical papers on the subject. Starkman et al (1966) studied spark-ignition (SI) application exclusively. Gray et al. (1966) studied compression-ignition (CI) application exclusively. While Pearsall and Garabedian (1967) studied both SI and CI applications.

### **2.3.2.1 Ammonia as a Spark-Ignition Engine Fuel**

Spark-ignition engine tests were performed on a single cylinder cooperative fuel research (CFR) engine by Starkman et al. (1966). Compression ratios were varied from 6:1 to 10:1. Ammonia was drawn from a high-pressure bottle stored in a hot water bath which had a maintained temperature by using submerged steam. Ammonia flow rate was measured and calibrated with a volumetric sight glass attached to the ammonia bottle. Continuous flow rate measurements were made with a turbine flow meter and automatic counter. Suitable regulators and needle valve were installed to reduce the line pressure and meter ammonia flow. Introduction was a simple standpipe into the intake.

Starkman et al. (1966) demonstrated that in order to combust anhydrous ammonia as a fuel in a SI engine, the ammonia must be introduced as a vapor and be partly decomposed into hydrogen and nitrogen with the minimum ammonia decomposition being 4-5% by weight of ammonia. Ammonia decomposition was accomplished by running the ammonia fuel stream through an electrically heated stainless steel catalyst chamber which was loosely filled with a pelletized activated iron catalyst.

Spark timing was advanced in order to operate ammonia but was on par with the sensitivity of hydrocarbon fuels. Increased cylinder wall temperature also aided in successful stable combustion.

Starkman et al. (1966) calculated that the maximum theoretical possible indicated output using ammonia could be up to 77% of a hydrocarbon based fuel. However, only 71% output was achieved experimentally using a compression ratio (CR) of 10:1, and only 62% output was achievable with a CR equal to 6:1. The brake specific fuel consumption (BSFC) increased two-fold at maximum power and 2.5 fold at maximum fuel economy.

The authors believe it is almost certain that the decomposition of ammonia takes place during compression. This decomposition then produces a form of hydrogen and its corresponding intermediate species. Thus as the compression ratio and combustion temperature are increased, so is the concentration of hydrogen being formed. The authors also believe that the oxidation kinetics of ammonia involves steps which produce non-equilibrium quantities of NO<sub>x</sub>. The rate of decomposition of NO<sub>x</sub> to N<sub>2</sub> and O<sub>2</sub> cannot take place, as assumed to yield equilibrium quantities predicted by theoretical calculations.

Maximum nitric oxide (NO) concentrations observed were about 4800 ppm using ammonia as compared to 3400 ppm using iso-octane (i-C<sub>8</sub>H<sub>18</sub>). Maximum power produced 3000 ppm NO using ammonia and 500 ppm NO using iso-octane. NO measurements were made using ultraviolet spectroscopy and nitrogen dioxide (NO<sub>2</sub>) deoxidized to NO.

The authors also calculated that the output of liquid ammonia injected directly into the cylinders could exceed that of a hydrocarbon fuel, but the high rate of vaporization of ammonia would be a difficult design hurdle.

### **2.3.2.2 Ammonia as a Compression-Ignition Engine Fuel**

Before major engine testing was performed, Gray et al. (1966) conducted material tests away from the engine. In these tests cast iron samples experienced a slight weight gain and discoloration. This was believed to be the effect of corrosion and seemed to increase with the excess exposure to  $\text{NO}_2$  and water. This could be a future design concern since these chemicals were formed increasingly in the exhaust as the air/fuel ratio deviated from stoichiometric. Aluminum samples also seemed to experience slight weight gain as well, but lacked discoloration.

When experiments were conducted during engine operation involving the introduction of  $\text{N}_2\text{O}$  and  $\text{NO}_2$  into the intake along with liquid ammonia introduced directly in the cylinder, noticeable corrosion of the intake manifold and combustion chamber were observed. This was believed to be caused by the acids formed by the combination of moisture in the air with the nitrogen based gaseous fuels. The cast-iron piston rings appeared to suffer no deterioration upon examination after engine operation. The babbit bearings seemed to experience the most noted overall weight change after engine operation, however, it too was quite small.

The copper lead bearing surfaces appeared to have the greatest visual change. The sintered copper-lead surface appeared to have a heavy tarnish-like oxidation and a pitted – type corrosion on the cast copper-lead bearing. It is believed by the author that if the tests were to have been conducted for a longer time the bearings would have been much worse. Bearing weight loss was also observed, but appeared to be on the same or less magnitude when compared to conventional hydrocarbon fuels.

Bearing weight loss was interesting in this case. In the case of hydrocarbon fuels, bearing weight loss seemed to occur as an exponential function with time increasing very rapidly once substantial corrosion has occurred. However, while using ammonia, the majority of weight loss occurred in the first 40 hr time interval. It was deemed that heavy tarnish provided some sort of protective coating to the bearing.

The effect of ammonia on neoprene and rubber seemed to be the harshest of all materials examined. Side effects included weight-change, swelling, loss of shape, and even disintegration. In the end, all materials except neoprene, rubber, copper, would be suitable for ammonia combustion use.

Oil samples were taken at every 40-hr interval and no changes were noted to the composition or properties of the REO-145 oil used. At the completion of the 120-hr mark, the deterioration level of the oil was less than that of a gasoline engine.

Similar to the Starkman et al. (1966) study, Gray et al. (1966) used a single cylinder CFR engine which was operated in both CI and SI modes. Gray et al. (1966) first began studies using a CI scheme with liquid ammonia injected directly into the cylinder. In order to first achieve the pressure, temperature and time conditions needed to ignite ammonia due to compression, the compression ratio of the engine was raised to 35:1, and jacket and intake air temperatures were raised to 150 °C. It was found when using these same engine operation characteristics the compression ratio could be lowered to as much as 30:1 at which point combustion ceased. Engine operation occurred at a speed of 900 rpm. Combustion was maintained throughout the injection timing range of 90-70 deg before top-dead-center

(BTDC) and ammonia flow rates of 2-5 lbs/hr. Using ammonia only, ignition delay increased slightly with increased engine speed.

Early injection timing and the high rate of vaporization of ammonia seemed to indicate that the air-fuel mixture in the cylinder was close to homogeneous at all times. However, ammonia did not seem to maintain a heterogeneous combustion scheme as demonstrated in classical diesel combustion.

In order to minimize the need for such a high compression ratio (high ignition energy), needed to combust ammonia only, other various techniques were investigated. These included: pilot injection, fuel additives, various pilot fuels, and glow plugs.

In comparison to the Starkman et al. (1966), Gray et al. (1966) noticed that at the optimum compression ratio and wide open throttle (WOT), hydrogen had no beneficial effect on combustion.

Primary pilot injection experiments were conducted using diesel fuel with a cetane number (CN) equal to 53 (a higher CN implies that the fuel is easier to autoignite). The compression ratio was lowered to 30:1. Air and jacket temperatures were adjusted to 65 and 100°C, respectively. For best combustion it was observed that ammonia must be injected no later than 40 deg before the end of diesel injection. No ammonia combustion was observed if the ammonia injection occurred after or slightly before the end of diesel injection. Maximum mean indicated mean effective pressure (IMEP) occurred when the end of injection of ammonia and diesel coincided and remained essentially constant as the ammonia injection was advanced before top-dead-center.

When compared to hydrocarbon fuels, injection timing was relatively more important than temperature for ammonia.

Gray et al. (1966) then proceeded to injecting ammonia as a gas into the intake stream. Local intake manifold air temperatures as low as  $-30^{\circ}\text{C}$  were observed when ammonia liquid was injected directly into the intake stream as a result of ammonia vaporization. A downside of injecting ammonia gas through the intake is that it displaces a portion of air, thereby decreasing the effective volumetric efficiency of the engine.

Pressure rises as much as 25 psi per crank angle degree (psi/deg), diesel ignition delay between 1-3 deg and more pronounced engine roughness were all observed when similar amounts of ammonia gas were introduced in the same manner as when ammonia was directly injected into the cylinder.

Grey et al. (1966) then experimented with other pilot fuels used in conjunction with gaseous ammonia injected into the intake under a CI engine operation scheme. In addition to diesel fuel, amyl nitrate (100+ CN) and dimethyl hydrazine (67 CN) were also used as pilot fuels. Dimethyl hydrazine was chosen since hydrazine made in the field much like ammonia, and dimethyl hydrazine is a safer laboratory substitute of hydrazine with the same combustion characteristics. In both cases combustion was readily achieved with the minimum compression ratios of 12:1 for amyl nitrate and 13.7:1 for dimethyl hydrazine. These results indicate that any fuel with a satisfactory cetane number may be used as a pilot injection fuel for ammonia.

Finally Gray et al. (1966) also experimented briefly with a specifically designed glow plug for an ammonia only combustion scheme. They observed that combustion was quite

sensitive to plug placement and ammonia flow rate. Combustion could also be maintained with a compression ratio as low as 23:1 and jacket and air temps of 100 and 65°C, respectively.

### **2.3.2.3 Ammonia as a Fuel in a Compression Ignition and Spark Ignition Application**

Two different approaches were used in the Pearsall and Garabedian (1967) study to demonstrate the feasibility of using anhydrous ammonia as a fuel. The first was demonstrated by supplying ammonia into the induction system and then causing compression ignition by a small pilot injection of diesel fuel. The second was by converting the compression ignition engine into a spark ignited engine and using no pilot fuel. The research engine used was a two cylinder version of a Continental AVDS-1790.

Direct injection of liquid ammonia was attempted but proved unsuccessful in this study, even with raising the CR to 30:1. The authors believe that the evaporation of the ammonia cooled the cylinder so much that a flame front could not be ignited. This was supported by the observation that the peak cylinder pressures dropped as much as 250 psi.

Diesel engines normally operate excessively lean because of smoke limitations. When operating under compression-ignition using a pilot injection, Pearsall and Garabedian (1967) observed that ammonia preferred to be operated closer to stoichiometric. Due to better air utilization they achieved power outputs running on ammonia that exceeded diesel only operation by as much as 32%. However, because of concern about the amount of torque that could be absorbed by the powertrain output for testing was reserved to diesel output ratings.

It was observed during testing that cylinder head temperature had a drastic affect on repeatability of fuel consumption and output. As cylinder head temps increased so did output. BSFC did the opposite.

The above study tried to minimize pilot diesel fuel flow as much as possible. Diesel flow was decreased so dramatically problems arose with cooling the injector tips, which in turn, caused clogging and lacquering. Daily cleaning was implemented to reduce this affect.

In all runs fuel injection timing and CR were held constant. Optimum ammonia flow proved to be a linear function of manifold pressure, since engines typically want to run at a constant equivalence ratio. However, the start of ignition became more retarded as manifold pressure decreased. Diesel fuel flow behaved inversely. Below 15 inHg of manifold pressure, the engine was not self-sustaining due to ignition lag. The increased ignition lag was assumed to be due to the decreased density of charge and the greater difficulty for diesel fuel to react with air. Small amounts of swirl appeared to have little effect on combustion characteristics.

Neither military compression-ignition and turbine engine fuel (CITE, 38 CN) or No. 2 diesel (44 CN) seemed to produce as positive results as No. 1 diesel (50 CN). The problems were late ignition, loss of power, and the inability to burn the same quantities of ammonia. With lower ignition quality fuel the engine demanded a much leaner air/fuel ratio (AFR).

Experiments to determine the effects of pilot fuel quantity proved that an increase in output and reduction of fuel consumption are directly proportional to the heat content of the additional diesel fuel. At leaner AFR the effect of increasing diesel pilot quantity was even

more dramatic. The increase of power output proved to be as high as three times the heat content of diesel fuel injected.

In general, the lowest brake specific fuel consumption (BSFC) of ammonia and a pilot fuel occurred in an equivalence ratio range of 0.7-0.75, whereas maximum output seemed to be at 0.9.

Pearsall and Garabedian (1967) then converted the engine from CI to SI by removing the injection pump and installing a magneto. The diesel injector was then removed and replaced with a 12mm spark plug. Three compression ratios were used 18.6, 16, and 12:1. Spark plugs with the longest reach obtainable were installed in order to optimize central flame location. Dropping compression ratio did little to reduce fuel consumption. Peak pressure dropped slightly (~100psi) for each CR step. BSFC was reduced by 6% at 12:1.

A direct comparison of performance between operation using a pilot fuel and operation using a supplied spark is difficult due to the different modes of testing. The compression-ignition configuration using pilot fuel could not be run by throttling the intake air because of high ignition lag. The spark ignition configuration could not be operated supercharged because of the limitation of available spark plugs.

With spark ignition, start of ignition is observed to be about 10 deg earlier. Peak cylinder pressure was observed to be about 500 psi higher and peak pressure occurred about 7 deg earlier. Output was higher than pilot ignition or straight diesel operation.

Neither the compression ratio or ignition source seemed to have an effect on the optimum AFR for best BSFC or output. The authors believed that SI engine operation

seemed to have an advantage over CI because it can be throttled at part load and there is no need for a secondary fuel.

It was noted by the authors, at the time of writing, ammonia was too expensive to economically compete with hydrocarbon fuels. However, in locations where these fuels would not be readily available, ammonia could be synthesized from another power station based source.

#### **2.3.2.4 Comparing the Army Papers**

When comparing the results of the Army-funded research, there seems to be only fundamental agreement on how to optimally operate an internal combustion engine on ammonia. Ammonia as a fuel needs a large amount of energy to cause ignition. This could either be from a spark plug in an SI application, or an extremely high compression ratio or small pilot fuel injection in CI applications.

Ammonia liquid injected directly into the cylinders theoretically provides the most output, but since ammonia has such a high rate of vaporization it cools the cylinder very effectively, and can cause unsustainable combustion.

Gray et al. (1966) disagrees with Starkman et al. (1966) that there is no need for ammonia dissociation prior to combustion in an SI application, but rather spark source location is a more important factor.

Ammonia seems to have little effect on engine materials except for bronze, copper, and rubber. All of these materials can easily be designed out of an engine with little price increase.

Only the Starkman et al. (1966) study acknowledged analysis of emissions from ammonia combustion. This can be understood because the studies occurred before exhaust emissions were of a major concern. However, it was observed by Starkman et al. (1966) that ammonia combustion provided a lower NO<sub>x</sub> output than some hydrocarbon fuels.

## **2.4 Ammonia as a Diesel Exhaust NO<sub>x</sub> Reducing Agent**

The only nitrogen-based post combustion species that are regulated are nitric oxide (NO) and nitrogen dioxide (NO<sub>2</sub>). When the concentrations of both of these species are combined they are more commonly referred to as nitrogen oxides (NO<sub>x</sub>), and are responsible for urban smog and some forms of acid precipitation (Caton and Xia, 2004). There are many methods that use ammonia, or other related nitrogen-based species, to remove NO<sub>x</sub> emissions from diesel engine exhaust.

### **2.4.1 Selective Catalytic Reduction (SCR)**

A diesel exhaust NO<sub>x</sub> reduction design scheme, that has roots in fossil fueled power plants, has become increasingly popular through research over the last decade is Selective Catalytic Reduction (SCR) (Alkemade and Schumann, 2006). SCR requires ammonia or urea to be injected into the exhaust downstream of combustion before a catalyst with a nominal temperature of 350 °C. The ammonia then reacts with NO in the presence of the catalyst to form molecular nitrogen and water (Javed, et al., 2007). The key reactions when using anhydrous or aqueous ammonia as an SCR reductant are as follows (Lambert, et al., 2006):



Using urea as a reductant has the benefit of being safer and easier to store than ammonia but requires conversion to ammonia through thermal decomposition in order to be used effectively. The equation for NO<sub>x</sub> reduction using urea is as follows:



SCR catalysts are manufactured from various ceramic materials used as carriers. These carriers are usually made of titanium oxide, oxides of base metals (such as vanadium and tungsten), zeolites, and/or other various precious metals. All catalyst components have their own unique advantages and disadvantages.

Base metal catalysts, such as the vanadium and tungsten, lack high thermal durability. They are less expensive and operate very well at the temperature ranges most commonly seen in industrial and utility boiler applications. Thermal durability is particularly important for automotive SCR applications that incorporate the use of a diesel particulate filter with forced regeneration. They also have a high catalyzing potential to oxidize SO<sub>2</sub> into SO<sub>3</sub>, which can be extremely damaging to the catalyst due to its acidic properties (Lambert, et al., 2006).

Zeolite catalysts have the potential to operate at significantly higher temperatures than base metal catalysts, with the ability to withstand long term operational temperatures of 650°C, and transient conditions of up to 850°C (Lambert, et al., 2006). This can be extremely important when used in conjunction with self cleaning diesel particulate filters. Recently developed iron and copper exchanged zeolite urea SCRs have been developed with

approximately equal performance to that of vanadium urea-SCRs if the fraction of the  $\text{NO}_2$  is 20% to 50% of the total  $\text{NO}_x$  (Gieshoff, et al., 2001).

Results have shown that urea is a slightly more effective reductant when using a CU-zeolite catalyst (Xu, et al., 2002). However, under steady state low temperature reaction conditions using ammonia performed better which was assumed to occur because of the possible incomplete hydrolysis of urea to ammonia below  $250^\circ\text{C}$  (Xu, et al., 2002). SCR has been shown to lower  $\text{NO}_x$  as much as 40% in a light-duty truck application (Lambert, et al., 2006).

#### **2.4.2 Selective Non-Catalytic Removal (SNCR)**

In general, combustion devices are designed to operate within a number of design constraints, and these constraints often have a drastic effect on the effective equivalence ratio at which the engine will operate. For example, gas turbines are operated with high ratios of excess air to ensure adequate cooling of the turbine blades. A medium-speed diesel engine is operated on a lean fuel mixture in order to ensure complete combustion. While most gasoline engines are operated near stoichiometric or rich conditions to achieve best power and fuel economy. In fact, oxygen levels can vary from less than 8% to over 21% by volume in any combustion (Caton and Xia, 2004) scheme, and it is these operating parameters that impose a design restriction on the exhaust after-treatment to be selected.

Selective Non-Catalytic Reduction is a post combustion process in which a nitrogen-based species is injected into diesel engine exhaust downstream of the engine in order to reduce end  $\text{NO}_x$  concentrations without the need for a catalyst. For most cases, SNCR is only effective over a narrow temperature range (Bowman, 1992). Reduction is poor at higher

temperatures because the reducing agent itself oxidizes to NO. Below optimum temperatures the reduction reactions are too slow and the reducing agent will be re-emitted without fully reacting, a condition known as slip. In existing combustion systems, random temperature gradients may vary with operating conditions, which places severe design constraints on the agent injection system which must disperse the chemical reagent evenly throughout the entire exhaust stream in order for it to mix with nitric oxides within the appropriate temperature range (Caton and Xia, 2004).

There are currently three main SNCR processes that are implemented: the thermal DeNO<sub>x</sub> process which uses ammonia (NH<sub>3</sub>), the RAPRENO<sub>x</sub> process which uses cyanuric acid ((HNCO)<sub>3</sub>), and the NO<sub>x</sub>OUT process which uses urea (NH<sub>2</sub>\*CO\*NH<sub>2</sub>) (Caton and Xia, 2004).

The first developed and published process is the Thermal DeNO<sub>x</sub> process which uses ammonia as the NO<sub>x</sub> reducing agent. Thermal DeNO<sub>x</sub> is an Exxon patented process developed in 1972 which involves the injection of ammonia into fuel lean combustion exhaust at very high temperatures (>1500°C) which was demonstrated by Kimball-Linne et al. In this process the ammonia may be injected as an aqueous solution or anhydrous, and is used primarily in exhaust streams from furnaces and burners from large boilers. Traditionally there have been concerns involving the handling, transportation, and storage of ammonia. There is also a tendency for ammonia slip across the reactor.

The RAPRENO<sub>x</sub> process uses solid cyanuric acid as its primary reducing agent. Solid cyanuric acid, which sublimates at temperatures above 920°C, is injected into hot exhaust gas and allowed to form gaseous isocyanic acid (HNCO). This isocyanic acid initiates a series of

reactions for appropriate conditions which result in the reduction of NO<sub>x</sub>. This process was first proposed Perry and Siebers (1986). One negative characteristic of this process is the possible excess production of nitrous oxide (N<sub>2</sub>O). Although all three processes may produce N<sub>2</sub>O, RAPRENO<sub>x</sub> produces the most by comparison (Caton and Xia, 2004).

The NO<sub>x</sub>OUT process uses urea as its main reduction agent as demonstrated by Arand et al. In this process typically either solid urea or a urea solution is injected into hot exhaust gas and allowed to decompose into HNCO and NH<sub>3</sub> under certain conditions using the following reaction (Caton and Siebers, 1989):



For these reasons, the NO<sub>x</sub>OUT process has been described as a combination of the ammonia based Thermal DeNO<sub>x</sub> and the cyanuric acid based RAPRENO<sub>x</sub> processes. As discussed by Jodal et al. (1990) the thermal breakdown of urea at temperatures above 970°C may lead to the formation of NH<sub>2</sub> and NCO radicals, and H<sub>2</sub> molecules in equal proportions. Alternatively, urea has been found to decompose into biuret (NH<sub>2</sub>CO(NH)CONH<sub>2</sub>) under different conditions (Muzio, et al., 1990).

A number of factors can affect the overall performance of the SNCR process. These include exhaust oxygen content (equivalence ratio), the chemistry kinetics of the reducing agent, mixing effectiveness of the reagent with the exhaust stream, non-uniform exhaust temperatures, and other possible catalytic reactions. On top of this, the exhaust chemistry is affected by the chosen specific reduction agent, temperature, pressure, existing exhaust species concentrations, and the allowed residence time. Some specific features of the

chemistry that are of importance are: the ratios of the reduction agent to NO<sub>x</sub> concentration, and the exhaust's oxygen/carbon monoxide/water concentrations (Caton and Xia, 2004).

The chemistry for these processes is complicated. These reactions depend highly on radical formation, which are responsible for generating the necessary reactions capable of reducing NO<sub>x</sub> and keeping the reactions self-sustaining (Miller, 1996).

As mentioned earlier engine exhaust content is extremely important in selecting the most effective exhaust after-treatment. For engines that have a low equivalence ratio (higher levels of oxygen) the RAPRENO<sub>x</sub> process may be the most effective. For engines such as automobile engines that operate with equivalence ratios close to unity (lower levels of oxygen) the Thermal DENO<sub>x</sub> process may be the best. And for combustion that operates between these ratios the NO<sub>x</sub>OUT method may be the most suitable choice. However, for all three processes, the reactions must occur in a temperature range between 1420-1600°C (Caton and Xia, 2004), which is a hard temperature to maintain under normal operating conditions. This then presents a need to heat the exhaust products, include a catalyst, or burn the reagent directly during combustion.

### **2.4.3 Discussion on Post Combustion NO<sub>x</sub> Removal**

SCR and SNCR methods provide a “simplicity” benefit to designers because they are both post combustion NO<sub>x</sub> removal techniques. The additional equipment needed may be easily attached to an already operating engine or combustion process. This eases integration but drives up cost. SNCR does not require a physical catalyst but does share the requirement of a reduction agent injection system.

Although both methods suffer from slip, SNCR must be more precisely controlled because there is no catalyst present to rid the exhaust of unreacted ammonia. However, because it requires no catalyst, exhaust temperatures must be higher. This will also drive up cost in materials that can handle and protect against excessive heat.

Another major problem that arises when trying to use SCR or SNCR is that each method must be tuned specifically to the combustion operation cycle it will compliment in order to produce the required amount of energy to activate the necessary chemical reactions. This becomes increasingly evident when an automotive application is considered. Design will require running numerous simulation cycles (both numerically and experimentally) in order to maintain maximum efficiency. The simulations can be run on a dynamometer or on an actual piece of equipment during its normal work day. But even the best two operators will not use the equipment in exactly the same way. Even when used for the same general purposes (i.e., a truck delivering goods to stores in a city), small differences in the route such as hills, one-way streets, amount unloaded, etc., can make the engine loads different enough that effectiveness of the system will suffer.

#### **2.4.4 Diesel NO<sub>x</sub> Reduction In-Cylinder**

Ammonia based catalytic and non-catalytic exhaust after-treatment methods suffer from many limitations such as narrow effective temperature range, short durability, and deposition of soot on the catalyst. However, another way to utilize ammonia as a NO<sub>x</sub> reduction agent is to inject it directly in cylinder after combustion. Miyamoto et al. (1995) demonstrated that injecting ammonia, and other similar species, directly into the cylinder after top-dead-center (ATDC), during the expansion stroke, provided a NO<sub>x</sub> reduction up to

60%. Using this method it was observed that ammonia concentrations in the exhaust were less than 10 ppm even with excess reagent being injected.

Direct injection in-cylinder overcomes the need for higher than normal exhaust temperatures needed for using nitrogen-based species as effective reduction agents, and injection ATDC (post combustion) assures that temperatures are not so high as to oxidize the reducer itself. Miyamoto et al. (1995) conducted research using a single cylinder, 4-stroke, swirl type diesel engine and tested three types of deoxidizing agents, ammonia, sodium acetate, and urea.

Overall urea provided the best NO<sub>x</sub> reduction with ammonia coming in second, and sodium acetate providing little more than straight water injection. An injection timing range of 50-100 crank angle degrees ATDC seemed to provide the best results. Although post combustion water injection provides cylinder cooling, it was observed that urea provided an additional deoxidizing effect. Stoichiometrically 1 mole of NH<sub>3</sub> reacts with 1 mole of NO, however it was observed experimentally, that 15 times more ammonia than NO had to be added to achieve maximum NO<sub>x</sub> reduction. With increasing engine speed, optimum urea injection timing advanced and NO<sub>x</sub> reduction decreased slightly, which was assumed to be due to decreased residence time in the cylinder. And minimum NO<sub>x</sub> reduction occurred with an equivalence ratio of 3.5 and increased with increasing air ratios.

## **2.5 Summary**

Besides being carbon-free ammonia has several desirable attributes. It has a high energy density, it is relatively easy to store, and it is one of the world's most synthesized

chemicals. However, its ignition temperature is relatively high at 650°C, and it must be combusted in concentrations of 16-25% by volume in air.

As early as World War II, people tried using ammonia as an alternative to fossil based fuels being consumed by the war effort (Koch, 1945). This led the U.S. Army to fund a series of experimental works to test the feasibility using ammonia as an alternative fuel source in the 1960's (Gray, et al., 1966; Pearsall and Garabedian, 1967; Starkman, et al., 1966). However, until the 1990's, not much work had been done on the subject, due to the low cost of petroleum based fuels (Broadmeadow and Ibrahim, 1995; Miyamoto, et al., 1995).

In these studies, it was shown that ammonia could provide sustainable combustion when used as a primary fuel or in conjunction with a pilot fuel or spark source in either spark-ignition and combustion-ignition combustion schemes. However, each method had its own advantages and drawbacks.

In order to combust ammonia in a CI engine the CR must be very high (approximately 30:1), or there must be a pilot ignition source available to provide sufficient ignition energy. It was shown that a spark ignition could sustain stable combustion with ammonia as a primary fuel but only approximately 70% output could be achieved. Experiments with both gaseous and liquid injection were attempted but gaseous injection proved to be the most effective and provide the most stable combustion.

Ammonia also has the potential to being a NO<sub>x</sub> reducing agent and several methods have been developed and proven successful. The first attempts of this were in the power generation industries and recently research has migrated to the automotive industry,

specifically in diesel fueled CI engines. Some success has been shown but new techniques are emerging and a winning horse has not been chosen.

The goal of this research is to investigate engine power, BSFC, in-cylinder pressure history, exhaust emissions, and oil degradation in order to assess the capabilities and characteristics of using anhydrous ammonia as a fuel in a multi-cylinder CI engine. Different fueling methods, and pilot fuels will also be investigated.

## **Chapter 3 Methods and Procedures**

This chapter summarizes the methods and procedures used to carry out this study. This chapter will describe the engine specifications and the required modifications to burn ammonia as a fuel, the instrumentation used, and the methodology behind calculations.

### **3.1 Engine System Design**

The first subsection describes the engine parameters. The second subsection describes the fueling system modifications that were made to the original equipment in order to introduce ammonia as a fuel.

#### **3.1.1 Engine Specifications**

For this study, tests were performed on a John Deere (Model 4045) multi-cylinder turbocharged diesel engine. Table 3.1 lists the engine specifications and operating conditions used in this study.

**Table 3.1 – Engine Specifications**

Engine Manufacturer	John Deere (JD)
Engine Model	4045TT068
Engine Serial Number	T04045T772802
Engine Type	In-line, 4-stroke
Bore and Stroke	106 x 127 (mm)
Total engine displacement	4.5 L
Firing Order	1-3-4-2
Compression Ratio	17.6:1
Piston Type	Bowl-in-piston
Valves per Cylinder Intake/Exhaust	1 / 1
Aspiration	Turbocharged
JD Turbo Part Number	RE59379
Injection System	Stanadyne DB4 Rotary Pump
JD Injection Pump Part Number	RE500617
Fuel Rate at Full Load Rated Speed	66.5-70.5 mm <sup>3</sup> /stroke
Peak Power @ 2100 rpm	66 kW / 88.5 hp
Peak Torque @ 1300 rpm	387 N-m / 285 ft-lb
Engine Testing Speed Range	1000 ~ 1800 rpm
Testing Load Range	5 ~ 100%
Fuel	Anhydrous Ammonia No. 2 diesel Biodiesel (B100)

### 3.1.2 Fuel System

Measurement of diesel fuel flow into the engine was completed gravimetrically using a scale that was accurate to the hundredth of a gram and a detached 10 gallon fuel cell. Total

fuel used was a simple subtraction of fuel weight before testing and fuel weight after the specified test time. The Stanadyne DB4 rotary injection pump was mechanically controlled and had an injection timing curve as shown in Figure 3.1.

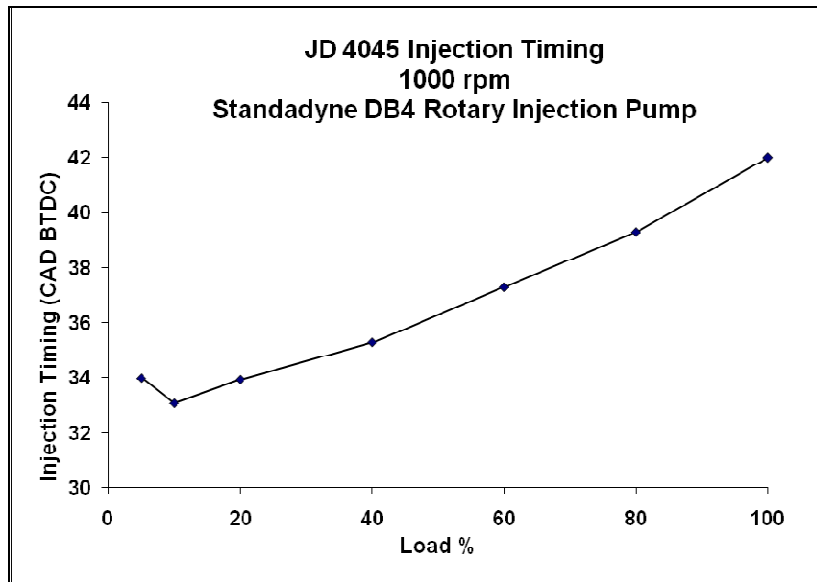


**Figure 3.1 – JD 4045 Stanadyne DB4 rotary injection pump timing map.**

In order to inject gaseous ammonia into the engine as a fuel, some modifications were required to the original engine intake setup. A 1/4 in. FNPT flush-mount pipe fitting was welded into the intake tube after the compressor before the intake manifold, as can be seen in Figure 3.2. A 3/8 in. outer-diameter (OD), 0.035 in. wall, stainless steel (SS) tube was then piped to the ammonia flow control system.



**Figure 3.2 – Ammonia intake location.**

### **3.1.1.1 Ammonia Flow Control System**

In order to effectively control the ammonia flow rate into the engine, a flow control system was developed using mechanical components and National Instruments LabVIEW software.

As seen in Figure 3.3, three 150 lb liquid storage ammonia tanks are connected together through a common manifold. Three tanks were used in order to lessen the draw on each specific tank and to null the effect of changing tank pressure as ammonia was used. It was observed in early testing that as ammonia was used, the tanks began to chill from the vaporization of liquid to gas. This caused the tank pressure to drop sufficiently and, over time, significantly reduce flow. The chilling was also believed to cause liquid ammonia condensation upon the tank needle valves and over time cause erratic readings and insufficient flow. The three tanks were stored in an outside location for safety reasons and

3/8 in. OD 0.035 in. wall SS tube connected the tank manifold to the ammonia flow control system.



**Figure 3.3 – Ammonia storage tanks.**

As seen in Figure 3.4, the tube from the tank manifold was connected to the flow control system. Upon initial connection the ammonia flows through a tee which has ball valves on both outlets. These ball valves provide a bypass loop around the control system in order to vent the lines at shutdown. With the bypass loop closed, ammonia is allowed to flow into the flow control system. This system utilizes a control ball valve, an on/off ball valve, and a replaceable orifice plate flow restrictor. The control valve is a variable position quarter-turn ball valve that utilizes a 12 V DC motor, controlled by LabVIEW software. The on/off ball valve is a two position (open/closed) 12V motorized valve that is also controlled by LabVIEW software. Both the control valve and on/off valves were products sourced from Raven Industries. The orifice plate flow (Figure 3.5) restrictor provides back pressure to the

flow control system, which allows better resolution with the control ball valve. The orifice plate flow restrictor was made from a TeeJet® Flow Restrictor, modified by welding a 3/8 in. NPT fitting on the outlet. The orifice plates were also sourced off-the-shelf from TeeJet®.

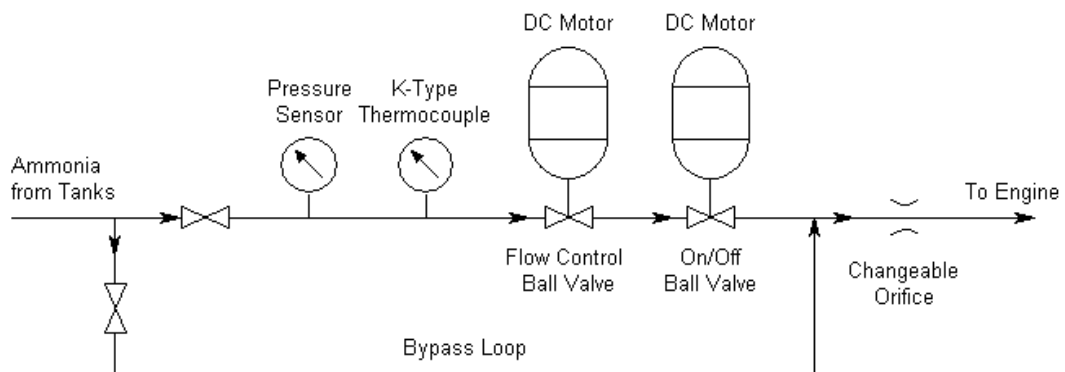
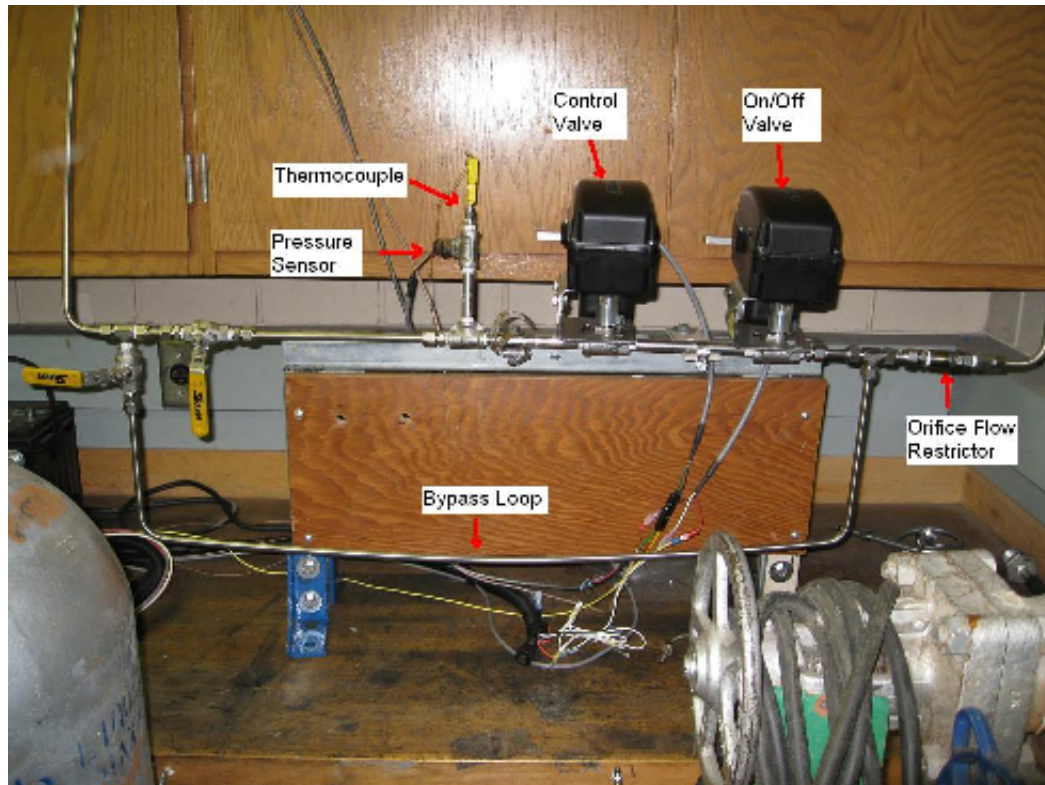


**Figure 3.4 – Ammonia fueling system.**



**Figure 3.5 – Orifice plate flow restrictor.**

In addition to the flow control system, in Figure 3.4, there is also a pressure sensor from Raven Industries and a K-type thermocouple. Both are located before the control valve.

The LabVIEW software program developed for the flow control system contains a closed loop algorithm that controls the engine torque +/- 5 ft-lb through the opening/closing of the mechanical control valve. All control parameters are inputted by the user.

Mass flow rate of ammonia into the engine was obtained gravimetrically by weighing the ammonia tanks before and after testing using a scale that was accurate to the tenth of pound. Although it was known not to be the most precise measurement, this method was chosen to be the best solution based on time, space, and budget constraints. Tests using ammonia were at least 20 min in duration to help promote accuracy. Future testing should find a more dynamic and accurate method for measuring intake ammonia flow rate.

Airflow into the engine was measured with a Meriam Instruments model 50MC2-4 laminar flow element. Its output is correlated to  $\text{inH}_2\text{O}$ .

### **3.2 Engine Testing Methods**

Once basic ammonia combustion had been achieved in the very early stages of testing, different engine operating schemes were designed. These methods will be described in the following sections.

### **3.2.1 Constant Peak Torque Testing**

The first engine testing method to be described is labeled as constant peak torque (CPT) operation, but first the definition of engine load must be established. Engine load percentage is a percentage of an established peak load. Peak load as defined in this study is the maximum attainable power at a given engine speed. Therefore, 20% load would be 20% of the engine's power at that speed. If the engine produced 100kW at a specific speed, then 20% load would be 20kW at that speed. This definition also carries through when operating on two fuels, i.e. diesel and ammonia.

In the CPT operation method, a specified amount of diesel load is achieved first and then ammonia is added on top to achieve 100% load at that test point. For example, in this operation mode, "20% diesel load" would comprise of 20% power from diesel fuel and 80% from ammonia. The same goes for "40% diesel load", 40% contributed power from diesel and 60% power contributed by ammonia.

### **3.2.2 Minimum Diesel Fueling with Variable Ammonia Flow Rates**

Another operation mode of interest was to use minimum diesel fueling combined with ammonia to achieve a part-load percentage. This gives the effect of ammonia being the primary fuel. In this mode of operation, the diesel fuel flow rate was maintained at a level that was equal to 5% of peak torque on diesel only operation. Then, the ammonia flow rate was adjusted to maintain the desired load percentage of its diesel only counterpart. For example, if the user desired a 20% loading condition while operating in the minimum diesel

fueling operation mode, 5% of the power would be from diesel fuel and the remaining 15% of the power would be from ammonia.

### **3.2.3 Test Fuels**

The ammonia used for testing was basic farm grade anhydrous ammonia.

The pilot fuel used while testing under both modes of operation included No. 2 diesel and biodiesel (B100). However, diesel fuel was the primary fuel for this study. Results when using B100 are labeled as such.

## **3.3 Engine Parameter Measurement and Analysis**

This section describes the methods and calculation techniques used in this study to determine how ammonia performed as a fuel in the areas of exhaust emissions, power, efficiency, brake specific fuel consumption (BSFC), and in-cylinder combustion pressure.

### **3.3.1 Ammonia Concentration Measurement**

In order to test ammonia concentration in the exhaust stream, a modified version of EPA test procedure CTM-027 was used (Environmental Protection Agency, 1997). The sample extraction equipment used was also derived from a sampling train labeled as Method 17 as found in *EPA Quality Assurance Handbook for Air Pollution Measurement Systems*, Volume III – *Stationary Source Specific Methods*, Section 3.11, January, 1982 (EPA-600/4-77-027b).

### 3.3.1.1 Ammonia Concentration Measurement Equipment

A sampling probe was located in the exhaust stream, as shown in Figure 3.6. The probe was constructed from a piece of 3/8 in. OD 0.035 in. wall SS tubing with 1/8 in. holes drilled in a line every 1/2 in. for approximately 4 in. in total length. The same procedure was then used every 90 degree around the probe with a 1/4 in. offset. Using a compression fitting the probe was inserted into exhaust pipe horizontally and attached by a bung weld fitting. The probe length was cut so that the probe tip was approximately 1/2 in. from the opposite side of the exhaust pipe. The tip of the probe was then crosscut with a 45 degree angle that would protrude perpendicular to the exhaust stream flow, as seen in Figure 3.7.

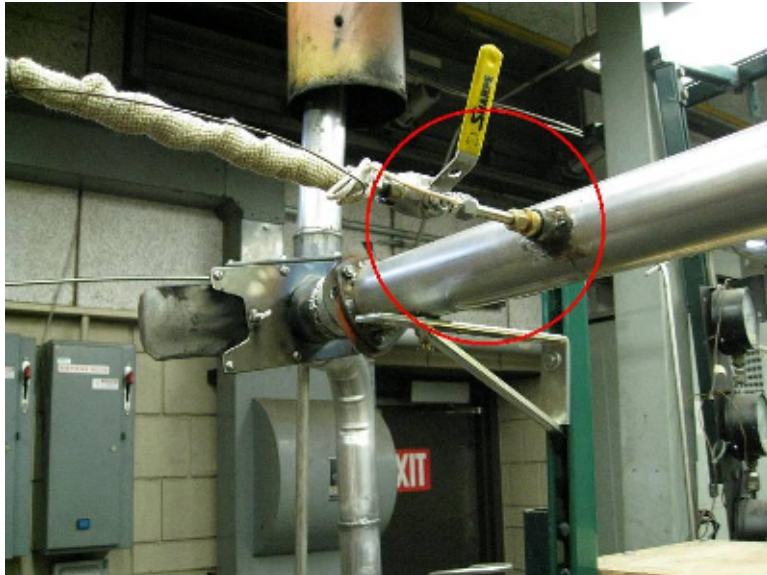


**Figure 3.6 – Ammonia concentration sampling probe location.**



**Figure 3.7 – Sampling probe.**

The exhaust probe was then connected to the ammonia sampling train via a heated 3/8 in. OD 0.035 in. wall SS tube, as shown in Figure 3.8. Early versions of the sampling train contained a particulate filter (Balston 58N with 100-12 Grade 404 Microfibre Filter Cartridge) and a non-heated line. Early testing showed that ammonia concentration measurement is very sensitive to water condensation. This conclusion was also confirmed by Shah (2007). In order to avoid this response, the sample line was heated and the particulate filter removed.

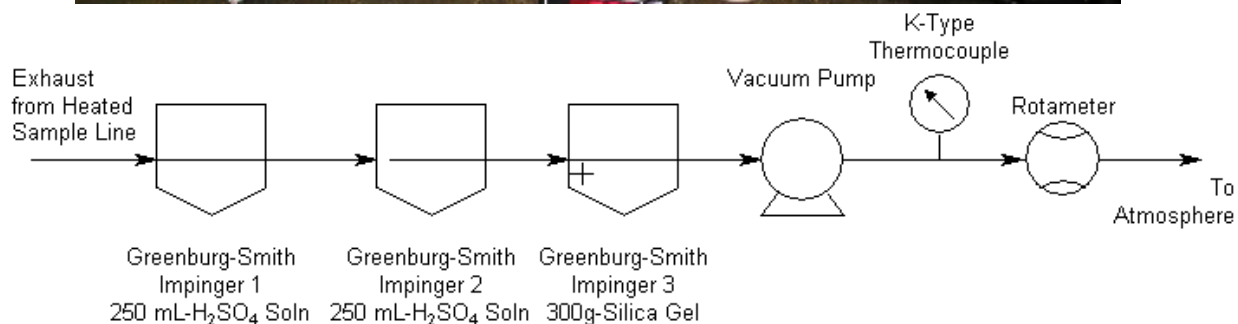
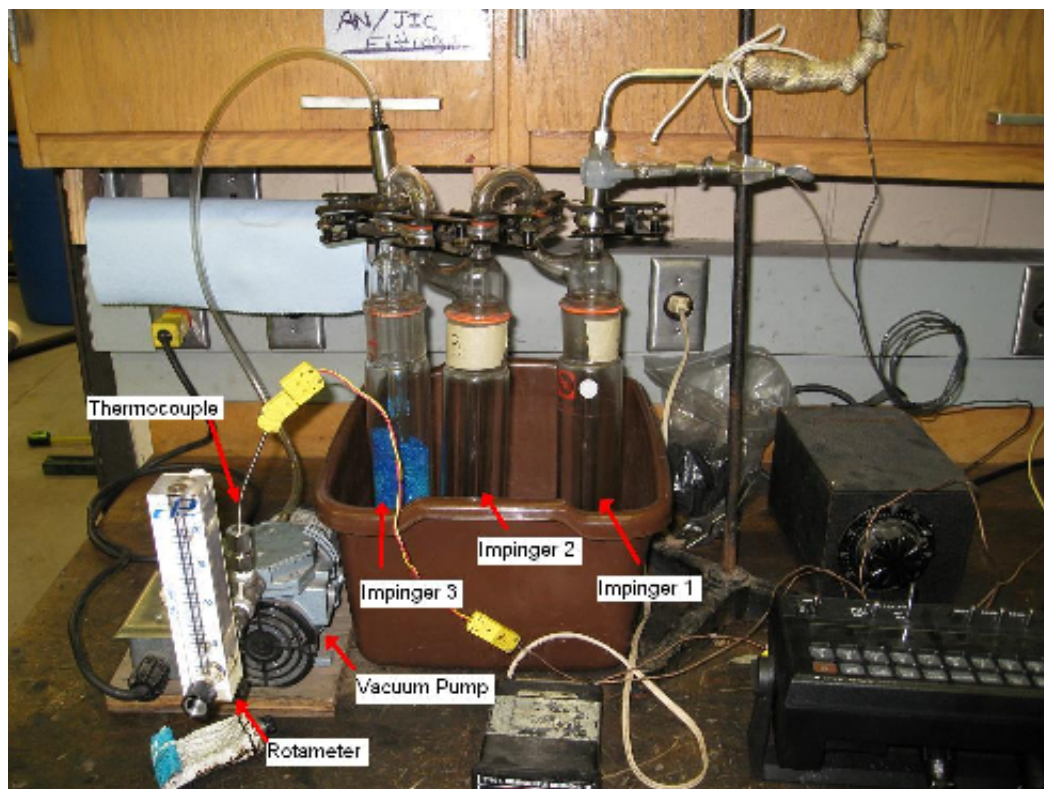


**Figure 3.8 – Ammonia concentration sampling train.**

The sample train consisted of three modified Greenburg-Smith impingers (no tapered tip) sitting in an ice water bath. The first two impingers contained 250mL of 4mL of H<sub>2</sub>SO<sub>4</sub> diluted in 1L de-ionized water (4mL/L solution). The third impinger contained approximately 300g of mesh 6-16 silica gel. The impinger train was then connected by 1/4 in. ID Tygon® tubing to a Gast Model MOA-P122-AA 4Z206 vacuum pump with a Cole Palmer rotameter

attached to the outlet side. The rotameter was calibrated in units of 0-20 liter per minute (LPM) air. A K-type Omega thermocouple was located in a tee between the rotameter and vacuum pump to measure the temperature of the outgoing flow.

### **3.3.1.2 Ammonia Concentration Measurement Procedure**

In order to test the ammonia concentration in the exhaust stream, the engine was brought to steady state. The first two impingers were filled with fresh 250mL of 4mL/L solution. The isolation ball valve and vacuum pump switch were turned on simultaneously. Each test had a 20-minute duration. Temperature measurements were recorded at 0, 10, and 20 minute intervals. A measurement of the flow rate going through the rotameter was also recorded at 10 minutes.

After the test was completed each impinger was dumped into a 500mL Nalgene sample bottle and labeled. Samples were then sent to a lab in order to be analyzed by the USEPA Method 350.1 for detecting Ammonia-N. This method uses alkaline phenol and hypochlorite to react with ammonia to form indophenol blue. The blue color formed is then intensified by sodium nitroprusside and measured spectrophotometrically at 650-660 nm. The above procedures were completed using a SEAL AQ2 discrete analyzer with test and reagent parameters programmed for this application. Results were reported in mg Nitrogen found in the 250 mL solution for each impinger (mg N/250mL).

The method used to calculate ppmV of ammonia present in the exhaust stream is derived from the EPA calculation method (section 4.3 page A-8), where:

$$N \left[ \frac{mgNH_4}{L} \right] = \left( C_1 \left[ \frac{mgN}{250mL} \right] + C_2 \left[ \frac{mgN}{250mL} \right] \right) * \frac{18.04}{14.01} * 2 \quad (3.1)$$

$N$  = Sum of concentrations of ammonium ion in all impingers

$C_1$  = Amount of nitrogen present in impinger 1

$C_2$  = Amount of nitrogen present in impinger 2

$18.04$  = Molecular weight of ammonium

$14.01$  = Molecular weight of nitrogen

$2$  = Conversion factor used to multiply total of 500mL collected solution to 1 L

$$V_a [L] = \frac{N \left[ \frac{mgNH_4}{L} \right] * 0.25 * 24.04}{1000 \left[ \frac{mg}{g} \right] * 18.04} \quad (3.2)$$

$V_a$  = Volume of ammonia gas in the sample of gas taken from exhaust

$0.25$  = Conversion factor, sample in impinger was contained in 0.25L solution (250mL)

$24.04$  = Liters of ideal gas per mole of substance

$1/1000$  = Factor to convert mg/L to g/L

$$V_{std} [L] = \dot{V}_m \left[ \frac{L}{min} \right] * 20 [min] * \frac{T_{std} [^{\circ}F]}{T_{avg} [^{\circ}F]} \quad (3.3)$$

$V_{std}$  = Volume of gas sampled measured by Rota meter corrected to standard conditions

$\dot{V}_m$  = Volumetric flow rate measured from rotameter

$20$  = Duration of test in min

$T_{std}$  = Standard temperature, assumed to be 77

$T_{avg}$  = Average temperature from measurements made at 0,10, and 20 minutes

$$NH_3 ppmV_{exh} = \frac{V_a [L]}{V_m [L]} * 10^6 \quad (3.4)$$

$$\dot{m}_{NH_3,exh} \left[ \frac{kg}{hr} \right] = \frac{V_a [L]}{V_m [L]} * \frac{\left( \dot{m}_{NH_3,int} + \dot{m}_{air} + \dot{m}_f \right) \left[ \frac{kg}{hr} \right]}{MW_{exh} \left[ \frac{kg}{kmol} \right]} * 17.03 \left[ \frac{kg}{kmol} \right] \quad (3.5)$$

$MW_{exh}$  = molecular weight of exhaust, method described in the next section

$\dot{m}_{NH_3,int}$  = mass flow rate of ammonia into the intake as measured

$\dot{m}_{air}$  = mass flow rate of air into the engine, method described in the next section

$\dot{m}_f$  = mass flow rate of pilot fuel as measured

17.03 = molecular weight of ammonia

Ammonia exhaust emission calculated as a function of engine power:

$$NH_3 \left[ \frac{g}{kW * hr} \right] = \frac{\dot{m}_{NH_3,exh} \left[ \frac{kg}{hr} \right]}{P_{both,avg} [kW]} \quad (3.6)$$

$P_{both,avg}$  = average power of engine while operating with both diesel and  $NH_3$

Final  $NH_3$  ppmV and  $NH_3$  g/kW-hr averages were plotted for each testing scheme versus load as can be seen in the results section.

### 3.3.2 Gaseous Emission Analysis

Three gases are held world wide as the regulatory standards for diesel exhaust gas emissions measurement. These gases are carbon monoxide (CO), hydrocarbons (HC), and

nitrogen oxides ( $\text{NO}_x$ ). Two other gases are commonly measured and reported but are not regulated. These are carbon dioxide ( $\text{CO}_2$ ) and oxygen ( $\text{O}_2$ ). However, depending on upcoming legislation  $\text{CO}_2$  may become relevant.

The equipment used in this study to measure gaseous emissions concentration were a Horiba 7100-DEGR gas analyzer and a De Jaye model DJGAS 5 gas analyzer. The Horiba gas analyzer was first used to measure only CO,  $\text{CO}_2$ ,  $\text{O}_2$ , and HC because of its higher accuracy methods of measurement. The Horiba analyzer uses a flame ionized detector (FID) method to detect total HC content which is more responsive than other non-dispersive infrared (NDIR) methods. It was found through consultation with Horiba that ammonia present in the exhaust stream would poison the original  $\text{NO}_x$  converter material used in the chemiluminescent analyzer over the long term and affect short term dynamic measurement by introducing interference in the analyzer's converter and reactor. This led to using the De Jaye analyzer for  $\text{NO}_x$  measurement. The De Jaye analyzer utilizes a pod type electrochemical NO sensor to correlate  $\text{NO}_x$  measurement which was thought to be less susceptible to ammonia poisoning.

After some testing it was found that the electrochemical NO sensor used by the DeJaye analyzer was also easily poisoned. Horiba was then contacted again and it was decided that the Horiba analyzer would be used to measure NO. In order to prevent permanent harm to the analyzer the original  $\text{NO}_x$  converter material (COM-03) was replaced with COM-GC3, which is unharmed by ammonia. This allowed the analyzer to be used in NO only measurement mode. Using this mode allows the converter interference problem to be eliminated because the sample is not allowed to pass through the bench's converter and

reactor. This technique allows measurement of NO only and not NO<sub>2</sub>. Therefore total NOx measurement was not attainable. This decision was made due to lack of time and funding needed to develop an NH<sub>3</sub> scrubber needed to prevent converter interference and to allow NOx measurement as referenced by Shah (2007).

### 3.3.3 Exhaust Emissions and Engine Efficiency Analysis

The exhaust emission concentration calculations were calculated as shown below. Baseline calculations were performed for cases using diesel fuel only and are as follows. Calculations of exhaust emissions concentrations normalized to power with diesel only were in accordance with SAE standards J244 (1992) and J1003 (2002). NOx concentrations were calculated as follows:

$$NOx \left[ \frac{g}{kw * hr} \right] = \frac{[14.01 + 2 * 16.00]}{10^4} * \frac{\frac{NOxppm}{10^4} * \dot{m}_f \left[ \frac{g}{hr} \right]}{\left( 12.01 + \frac{H}{C} * 1.01 \right) * \left( \frac{COppm}{10^4} + CO_2\% + \frac{HCppm}{10^4} \right) * P[kW]} \quad (3.7)$$

$NOxppm$  = measured NOx concentration in ppm

$H/C$  = Hydrogen to carbon ratio of fuel, for diesel it is 1.78

$COppm$  = measured concentration of CO in ppm

$HCppm$  = measured concentration of HC in ppm

$\dot{m}_f$  = mass flow rate of fuel

$P$  = engine power

14.01 = molecular weight of nitrogen

16.00 = molecular weight of oxygen

12.01 = molecular weight of carbon

1.01 = molecular weight of hydrogen

Calculation of NOx relative to diesel fuel used:

$$NO_x \left[ \frac{g}{kg_f} \right] = \frac{NO_x \left[ \frac{g}{kW * hr} \right] * 1000 \left[ \frac{g}{kg} \right] * P [kW]}{\dot{m}_f \left[ \frac{g}{hr} \right]} \quad (3.8)$$

Calculation of NO concentration normalized to power with diesel only:

$$NO \left[ \frac{g}{kW * hr} \right] = \frac{[14.01 + 16.00] * \frac{NO_{ppm} \dot{m}_f \left[ \frac{g}{hr} \right]}{10^4}}{10^4 * \left( 12.011 + \frac{H}{C} * 1.01 \right) * \left( \frac{CO_{ppm}}{10^4} + CO_2 \% + \frac{HC_{ppm}}{10^4} \right) * P [kW]} \quad (3.9)$$

$NO_{ppm}$  = measured NO concentration

$CO_2\%$  = measured  $CO_2$  concentration

Calculation of NO relative to diesel fuel used:

$$NO \left[ \frac{g}{kg_f} \right] = \frac{NO \left[ \frac{g}{kW * hr} \right] * 1000 \left[ \frac{g}{kg} \right] * P [kW]}{\dot{m}_f \left[ \frac{g}{hr} \right]} \quad (3.10)$$

Calculation of CO concentration normalized to power with diesel only:

$$CO \left[ \frac{g}{kW * hr} \right] = \frac{28.01 * \frac{CO_{ppm}}{10^4} * \dot{m}_f \left[ \frac{g}{hr} \right]}{\left( 12.01 + \frac{H}{C} * 1.01 \right) * \left( \frac{CO_{ppm}}{10^4} + CO_2 \% + \frac{HC_{ppm}}{10^4} \right) * P [kW]} \quad (3.11)$$

28.01 = molecular weight CO

Calculation of CO relative to diesel fuel used:

$$CO \left[ \frac{g}{kg_f} \right] = \frac{CO \left[ \frac{g}{kW * hr} \right] * 1000 \left[ \frac{g}{kg} \right] * P [kW]}{\dot{m}_f \left[ \frac{g}{hr} \right]} \quad (3.12)$$

Calculation of HC concentration normalized to power with diesel only:

$$HC \left[ \frac{g}{kW * hr} \right] = \frac{\frac{HC_{ppm}}{10^4} * \dot{m}_f \left[ \frac{g}{hr} \right]}{\left( 12.01 + \frac{H}{C} * 1.01 \right) * \left( \frac{CO_{ppm}}{10^4} + CO_2 \% + \frac{HC_{ppm}}{10^4} \right) * P [kW]} \quad (3.13)$$

Calculation of HC relative to diesel fuel used:

$$HC \left[ \frac{g}{kg_f} \right] = \frac{HC \left[ \frac{g}{kW * hr} \right] * 1000 \left[ \frac{g}{kg} \right] * P [kW]}{\dot{m}_f \left[ \frac{g}{hr} \right]} \quad (3.14)$$

Calculation of molar fraction of H<sub>2</sub>O in exhaust:

$$x_{H_2O} = 1 - \left[ \frac{CO_2 \%}{100} + \frac{CO_{ppm}}{10^4} + \frac{HC_{ppm}}{10^6} + \frac{O_2 \%}{100} + 3.76 * \frac{O_2 \%}{100} + \frac{NO_{xppm}}{10^6} \right] \quad (3.15)$$

3.76 = ratio of N<sub>2</sub> to O<sub>2</sub> in air

Calculation of molecular weight of exhaust:

$$MW_{exh} \left[ \frac{g}{kmol} \right] = \frac{CO_2 \%}{100} * [12.01 + 16.00 * 2] + \frac{CO_{ppm}}{10^4} * [12.01 + 16.00] + \frac{HC_{ppm}}{10^6} * [1.01 + 12.01] \\ + \frac{O_2 \%}{100} [16.00 * 2] + 3.76 * \frac{O_2 \%}{100} * [14.01 * 2] + \frac{NO_{xppm}}{10^6} * [14.01 + 16.00] + x_{H_2O} * [1.01 * 2 + 16.00] \quad (3.16)$$

Calculation of density of exhaust:

$$\rho_{exh} \left[ \frac{kg}{m^3} \right] = \frac{p_{exh} [psia] * \frac{101.3 [kPa]}{14.7 [kPa]}}{\frac{R \left[ \frac{kJ}{kg * K} \right]}{MW_{exh}} * T_{exh} [K]} \quad (3.17)$$

$R$  = universal gas constant, 8.314

Calculation of volumetric airflow into engine:

$$\dot{V}_{air} \left[ \frac{m^3}{hr} \right] = 53.518 * DP [inH_2O] - 0.094278 * DP^2 [inH_2O] * \frac{181.8718}{\mu_f} * \frac{p_1 [psia]}{p_{std}} * \frac{T_{std}}{T_1} * 1.699 \quad (3.18)$$

$DP$  = measured differential pressure across laminar flow element

$p_1$  = Inlet air pressure

$p_{std}$  = atmospheric pressure, assumed to be 14.7 psia

$T_1$  = Inlet air temperature

$T_{std}$  = atmospheric temperature, assumed to be 25°C

$\mu_f$  = viscosity correction factor from formula, based on temperature

181.8718 = constant from formula

53.518 = constant from formula

0.094278 = constant from formula

Conversion of exhaust density:

$$\rho_{air} \left[ \frac{kg}{m^3} \right] = \frac{p_{int} [psia] * \frac{101.3[kPa]}{14.7[psia]}}{\frac{R \left[ \frac{kJ}{kg * K} \right]}{MW_{air}} * T_{int} [K]} \quad (3.19)$$

$P_{int}$  = intake pressure

$MW_{air}$  = molecular weight of air 28.96

$T_{int}$  = intake temperature

Conversion of mass flow rate of intake air:

$$\dot{m}_{air} \left[ \frac{kg}{hr} \right] = \rho_{air} \left[ \frac{kg}{m^3} \right] * \dot{m}_{air} \left[ \frac{m^3}{hr} \right] \quad (3.20)$$

Calculation of mass flow of exhaust:

$$\dot{m}_{exh} \left[ \frac{kg}{hr} \right] = \dot{m}_{air} \left[ \frac{kg}{hr} \right] + \dot{m}_f \left[ \frac{kg}{hr} \right] \quad (3.21)$$

Conversion of mass flow rate of exhaust:

$$\dot{V}_{exh} \left[ \frac{m^3}{kg} \right] = \frac{\dot{m}_{exh} \left[ \frac{kg}{hr} \right]}{\rho_{exh} \left[ \frac{kg}{m^3} \right]} \quad (3.22)$$

Calculation of mass air/fuel ratio:

$$mass \frac{A}{F} = \frac{\dot{m}_{air} \left[ \frac{kg}{hr} \right]}{\dot{m}_f \left[ \frac{kg}{hr} \right]} \quad (3.23)$$

After all baseline diesel only emissions tests were conducted and recorded, ammonia emissions testing began. Below are emissions calculations specific to a combination of ammonia and diesel while running constant peak torque and variable ammonia flow rate testing. All other calculations can be assumed to be the same as diesel only methods, with the exceptions of engine power ( $P$  [kW]) is now represented as the power produced from the combination of diesel and ammonia, unless otherwise stated, and  $\dot{m}_f$  is represented by  $\dot{m}_{tot}$ .

Calculation of total fuel flow when using ammonia and diesel:

$$\dot{m}_{tot} \left[ \frac{g}{hr} \right] = \dot{m}_{diesel} \left[ \frac{g}{hr} \right] + \dot{m}_{NH_3} \left[ \frac{g}{hr} \right] \quad (3.24)$$

Calculation of air/fuel ratio for ammonia and diesel:

$$mass \frac{A}{F} = \frac{\dot{m}_a \left[ \frac{kg}{hr} \right]}{\dot{m}_{tot} \left[ \frac{kg}{hr} \right]} \quad (3.25)$$

In order to calculate the power provided by diesel fuel only, a torque reading was taken before any ammonia was added. The calculation of the power added by the diesel fuel only when operating on both ammonia and diesel was as follows:

$$P_{diesel} [kW] = \frac{Tq_{diesel} [ft * lb] * N \left[ \frac{rev}{min} \right] * 0.7457 \left[ \frac{kW}{hp} \right]}{5252} \quad (3.26)$$

In order to calculate the power provided by ammonia fuel only, torque readings were taken in five minute intervals after ammonia was added in conjunction with diesel fuel during operation. These readings were then averaged over the span of the test. Calculation of the

power added by the ammonia fuel only when operating on both ammonia and diesel is as follows:

$$P_{NH3,avg} [kW] = \frac{(Tq_{both,avg} [ft * lb] - Tq_{diesel} [ft * lb]) * N \left[ \frac{rev}{min} \right] * 0.7457 \left[ \frac{kW}{hp} \right]}{5252} \quad (3.27)$$

Combustion efficiency as a function of volume, on a ppmV basis, while operating with ammonia as the primary fuel is described below. Molar flow rate of ammonia in the intake:

$$\dot{x}_{NH3,int} \left[ \frac{kmol}{hr} \right] = \frac{\dot{m}_{NH3,int} \left[ \frac{kg}{hr} \right]}{17.03 \left[ \frac{kg}{kmol} \right]} \quad (3.28)$$

Molar flow rate of air in the intake:

$$\dot{x}_{air} \left[ \frac{kmol}{hr} \right] = \frac{\dot{m}_{air} \left[ \frac{kg}{hr} \right]}{28.96 \left[ \frac{kg}{kmol} \right]} \quad (3.29)$$

Concentration of ammonia in the intake:

$$\dot{V}_{NH3,int} [ppmV] = \frac{\dot{x}_{NH3,int} \left[ \frac{kmol}{hr} \right] * 10^5}{\dot{x}_{NH3,int} \left[ \frac{kmol}{hr} \right] + \dot{x}_{air} \left[ \frac{kmol}{hr} \right]} \quad (3.30)$$

Combustion efficiency of ammonia on a volume

$$\text{basis: } \eta_{comb, ppmV} = 1 - \frac{\dot{V}_{NH3,exh} [ppmV]}{\dot{V}_{NH3,int} [ppmV]} \quad (3.31)$$

It was also decided to calculate combustion efficiency on a mass basis which is described below:

$$\eta_{comb, mass} = 1 - \frac{\dot{m}_{NH_3, exh} \left[ \frac{kg}{hr} \right]}{\dot{m}_{NH_3, int} \left[ \frac{kg}{hr} \right]} \quad (3.32)$$

### 3.3.4 Exhaust Particulate Matter Analysis

Exhaust particulate matter was measured using an AVL 415S Variable Sampling Smoke Meter. Measurements were recorded in  $mg/m^3$ . The results were then normalized to the engines power level. For diesel only operation the following calculations were used:

$$soot \left[ \frac{g}{kW * hr} \right] = \frac{soot_{meas} \left[ \frac{mg}{m^3} \right] * \dot{m}_{exh} \left[ \frac{m^3}{hr} \right]}{P[kW] * 1000 \left[ \frac{mg}{g} \right]} \quad (3.33)$$

$$soot \left[ \frac{g}{kg_f} \right] = \frac{soot \left[ \frac{g}{kW * hr} \right] * P[kW] * 1000 \left[ \frac{g}{kg} \right]}{\dot{m}_f \left[ \frac{g}{hr} \right]} \quad (3.34)$$

For engine operation with both diesel and ammonia the above calculations were used. However, power is represented by the power of the combined fuels.

### 3.3.5 Brake Specific Fuel Consumption Analysis

Brake specific fuel consumption (BSFC) on diesel only was calculated the following way:

$$\dot{m}_f \left[ \frac{mg}{stroke} \right] = \frac{\dot{m}_f \left[ \frac{g}{hr} \right] * 2 \left[ \frac{rev}{cycle} \right] * 1000 \left[ \frac{mg}{g} \right]}{60 \left[ \frac{min}{hr} \right] * n \left[ \frac{rev}{min} \right] * 4 \left[ \frac{stroke}{cycle} \right]} \quad (3.35)$$

$$BSFC \left[ \frac{g}{kW * hr} \right] = \frac{\dot{m}_f \left[ \frac{g}{hr} \right]}{P [kW]} \quad (3.36)$$

Brake specific fuel consumption with engine operating on both fuels was calculated the following way:

$$BSFC_{diesel} \left[ \frac{g}{kW * hr} \right] = \frac{\dot{m}_{f,diesel} \left[ \frac{g}{hr} \right]}{P_{diesel} [kW]} \quad (3.37)$$

$$BSFC_{NH_3} \left[ \frac{g}{kW * hr} \right] = \frac{\dot{m}_{f,NH_3} \left[ \frac{g}{hr} \right]}{P_{NH_3,avg} [kW]} \quad (3.38)$$

$$BSFC_{tot} \left[ \frac{g}{kW * hr} \right] = \frac{\dot{m}_{f,tot} \left[ \frac{g}{hr} \right]}{P_{both,avg} [kW]} \quad (3.39)$$

### 3.2.5 Cylinder Pressure Measurement

In order to measure cylinder pressure, the engine was fitted with a Kistler model # 6125A pressure sensor that was threaded directly into a hole that was specifically made in the cylinder head. The pressure sensor was then wired into a signal amplifier and recorded with a LabVIEW 8.1 DAQ card and its corresponding data acquisition software. Results were then analyzed and plotted for cylinder pressure, cylinder temperature, and heat release.

## Chapter 4 Results

### 4.1 Baseline Testing with Diesel Fuel

In order to compare results a baseline was established for the test engine. These baseline tests consisted of establishing engine power, torque, and brake specific fuel consumption (BSFC) curves for the engine speeds being considered. Results were gathered for 1000, 1400, and 1800 rpm and can be seen in Figures 4.1-4.3.

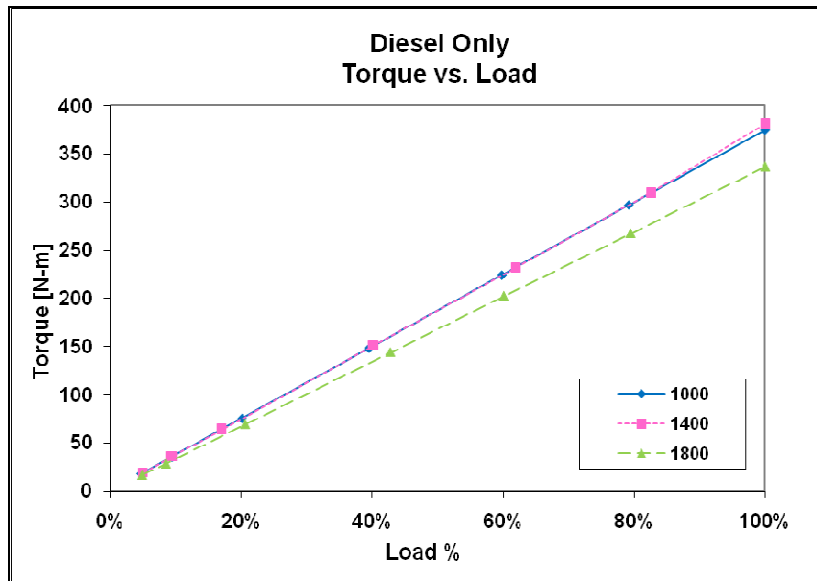


Figure 4.1 - Torque vs. load curves for diesel only operation.

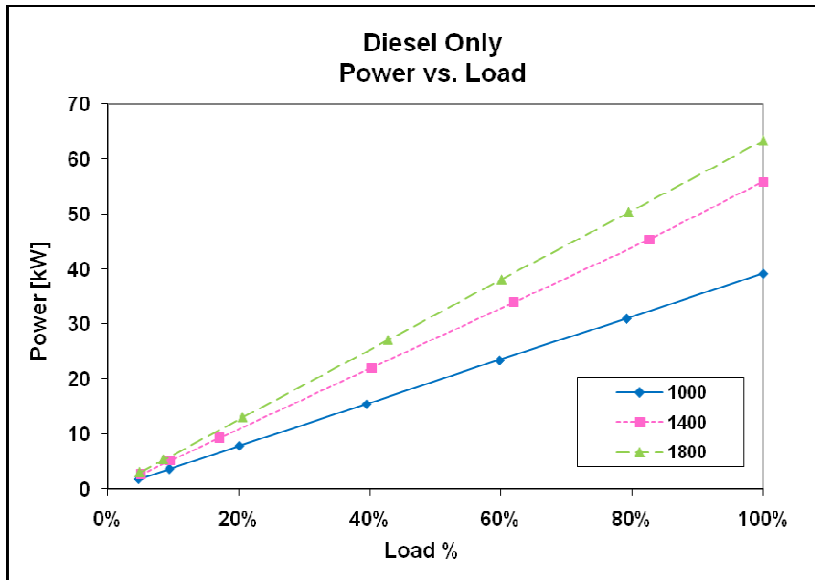


Figure 4.2 – Power vs. load curve for diesel only operation.

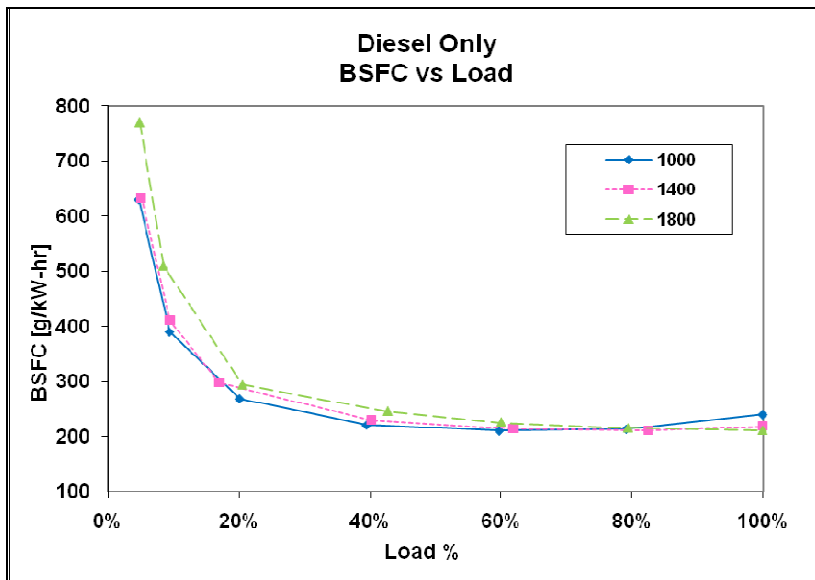


Figure 4.3 – BSFC vs. load curves for diesel only operation.

As can be seen from the BSFC curve there is poor combustion efficiency at low loads. This is a common occurrence with diesel and non-diesel engines that are not electronically controlled, because at low load the small amounts of fuel being delivered do

not atomize efficiently. In addition, overall combustion is relatively lean which can prevent complete combustion.

The next step in testing was to establish a baseline for emissions testing. Figures 4.4-4.8 show the emissions measured under diesel only operation for 1000 rpm.

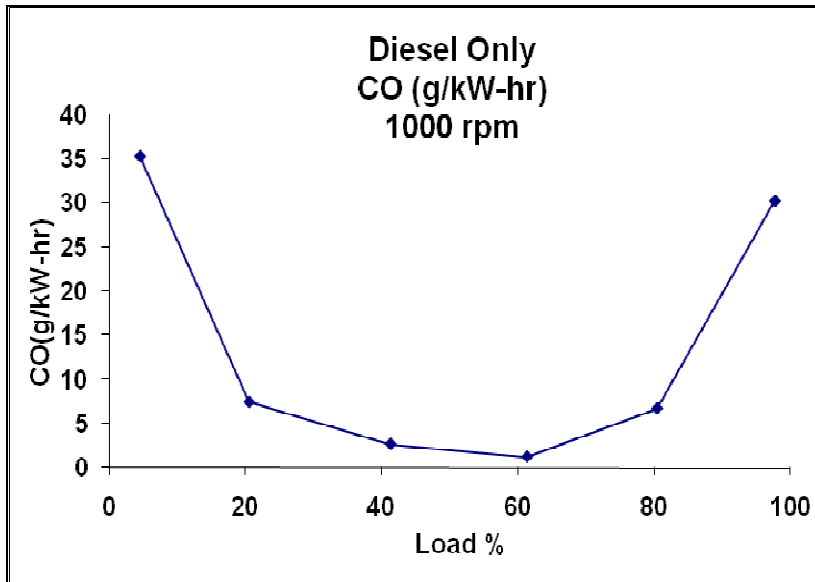


Figure 4.4 – CO emissions under diesel only operation.

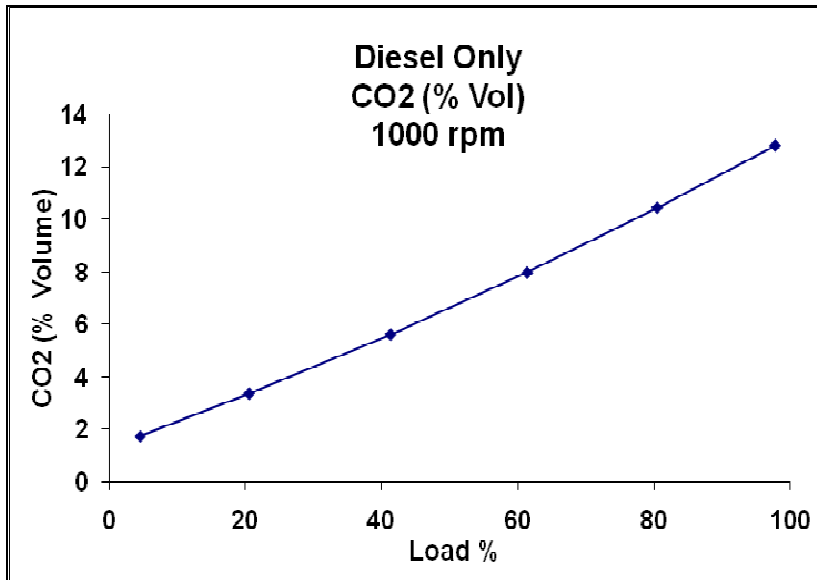


Figure 4.5 – CO<sub>2</sub> emissions under diesel only operation.

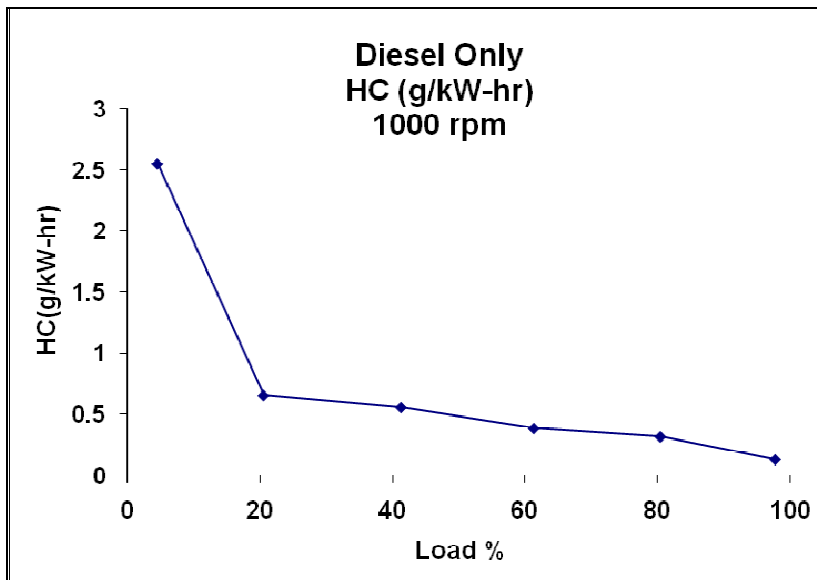


Figure 4.6 – HC emissions under diesel only operation.

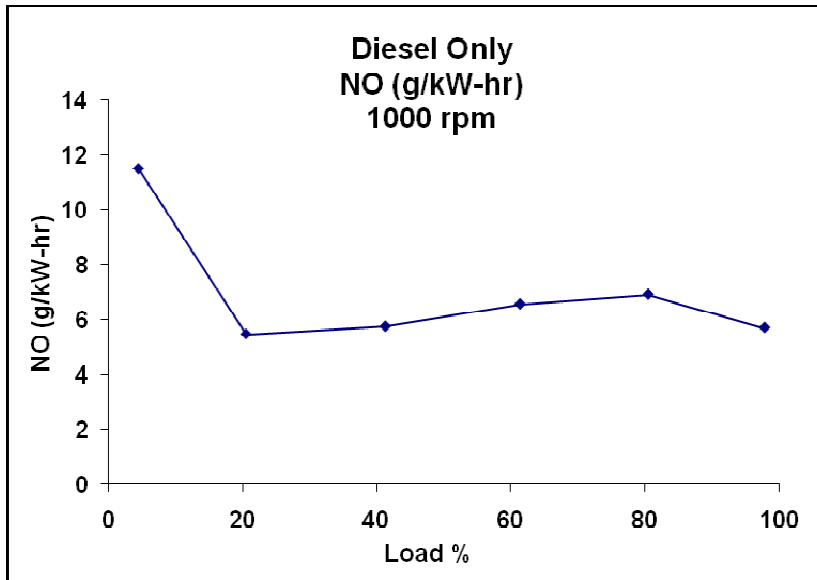


Figure 4.7 – NO emissions under diesel only operation.

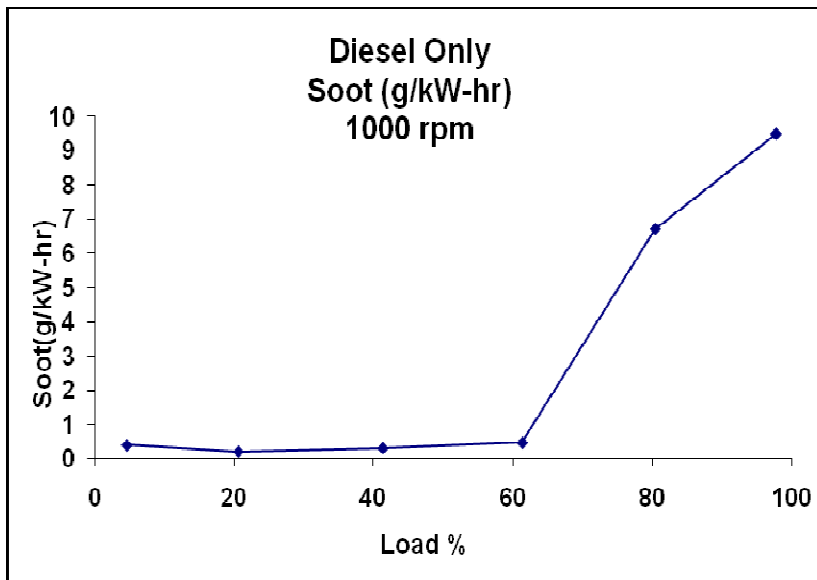


Figure 4.8 – Soot emissions under diesel only operation.

## 4.2 Testing with Ammonia and Diesel Fuel

The first ammonia combustion engine tests performed in this study were to demonstrate the feasibility of burning ammonia in the present diesel engine. Pressurized gaseous ammonia was fed into the intake manifold via a standpipe as described in Chapter 3. The test results (Figures 4.9 and 4.10) confirmed that a constant increase in engine torque could be obtained from the combustion of ammonia. The results showed an increase in engine torque over the entire load range. This confirmed that ammonia could be used as a fuel with little modification to the existing engine.

In order to fairly represent energy added by the ammonia, energy replacement calculations were performed by taking the total power of both fuels and subtracting the known power amount contributed by diesel only. This difference in power was taken as the power contributed by the ammonia.

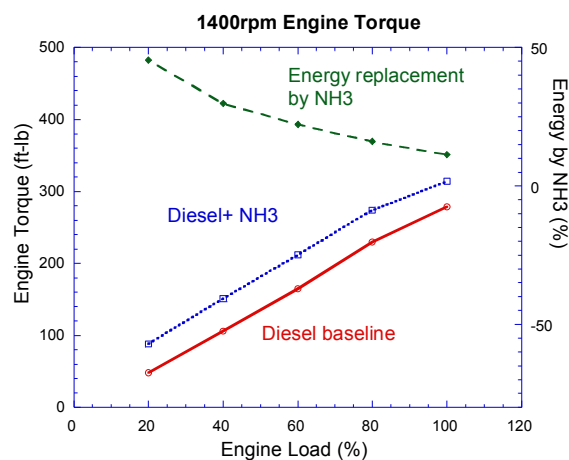
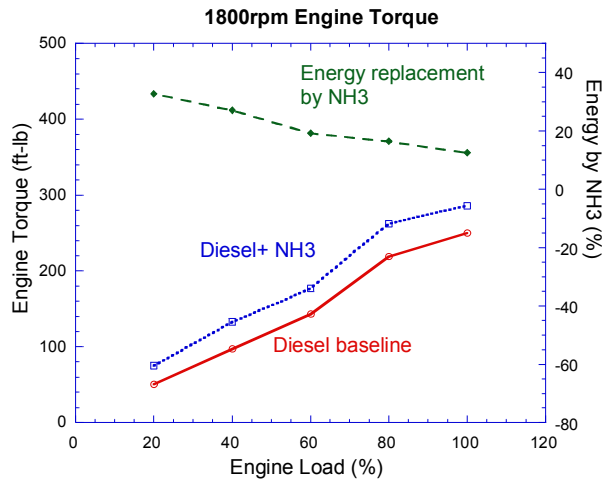


Figure 4.9 – Engine torque and energy replacement data while operating on ammonia and diesel fuel at 1400 rpm.



**Figure 4.10 – Engine torque and energy replacement data while operating on ammonia and diesel fuel at 1800 rpm.**

After many parametric tests were conducted, a decision was made to focus on results at 1000 rpm. This engine speed was deemed a safe operation point for the dynamometer measurement equipment and engine. All results, unless noted, will be presented for 1000 rpm.

#### 4.2.1 Constant Peak Torque Testing with Ammonia

The next step to evaluate ammonia as a viable fuel was to design different energy contribution methods in order to see how ammonia combustion would respond. One method of testing designed was to use ammonia in tandem with diesel fuel such that the total energy produced would be equal to the peak output of 100% diesel only operation. Experiments were conducted with different combinations of diesel and ammonia fueling. Under this method of operation, the diesel fuel flow rate was controlled so that the engine only produced

a specific percentage of the peak torque. Then, ammonia was added until the diesel only peak torque value was achieved.

The engine power/torque curves, brake specific fuel consumption (BSFC), and fuel flow rates for this “constant peak torque” testing method are shown in Figures 4.11-4.14. In general, the BSFC results for ammonia and diesel fuel have opposite trends with respect to the diesel load. For low diesel load (e.g., less than 15%), diesel BSFC is low due to the poor part-load efficiency as in a regular diesel engine. On the contrary, the ammonia BSFC can be maintained at a reasonable level. As the diesel energy increases beyond 60%, the amount of ammonia supplied to the engine is approaching its flammability limits and the premixed ammonia-air mixture in the cylinder is too lean to effectively sustain efficient flame propagation. Therefore, the ammonia BSFC is high, as can be seen in the BSFC curve for ammonia. In practice, operating points at either extremely high or low ammonia substitutions need to be avoided to prevent poor BSFC.

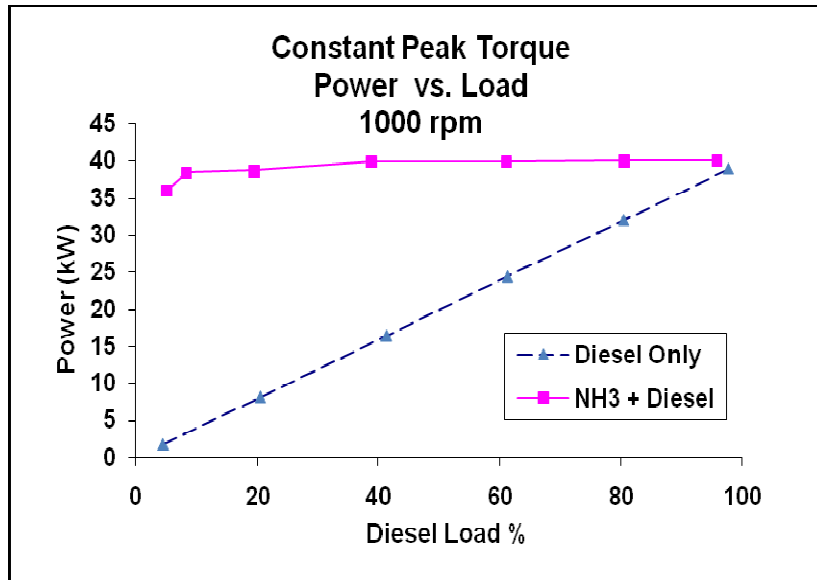


Figure 4.11 – Measured power output of engine under constant peak torque operation at 1000 rpm.

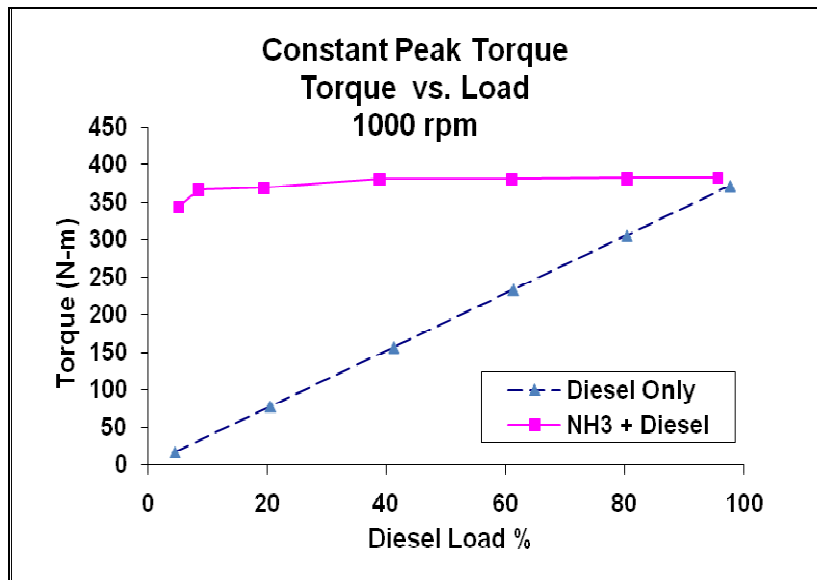


Figure 4.12 – Measured torque output of engine under constant peak torque operation at 1000 rpm.

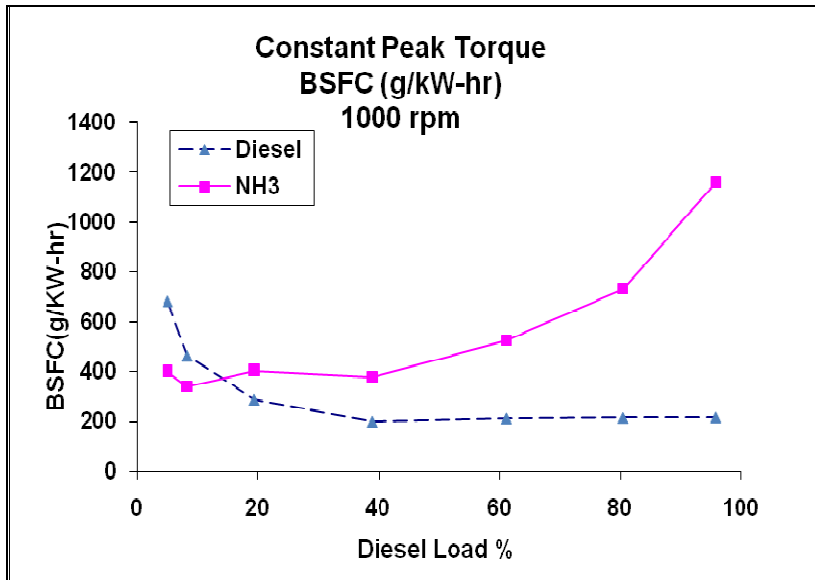


Figure 4.13 – Measured engine BSFC data under constant peak torque operation at 1000 rpm.

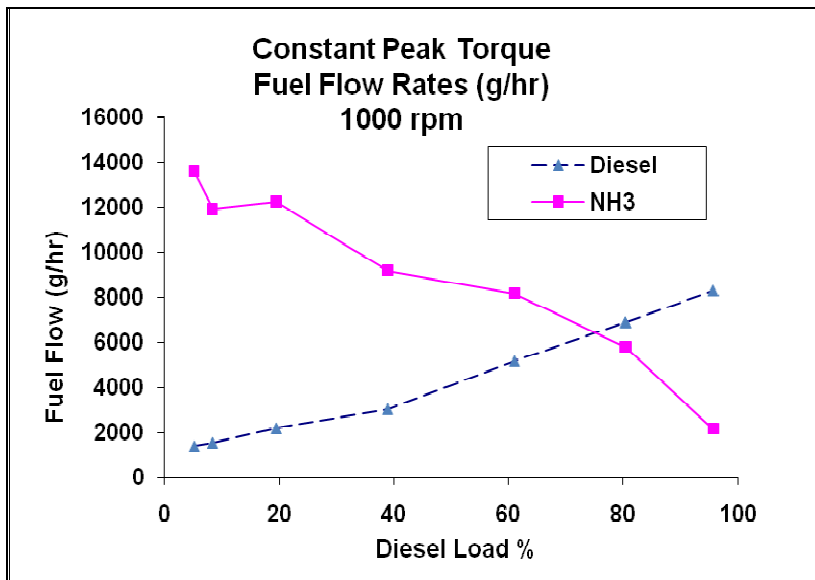


Figure 4.14 – Measured fuel flow under constant peak torque operation at 1000 rpm.

Exhaust emissions (CO, CO<sub>2</sub>, HC, NO and soot) were measured for constant peak torque operation and are shown in Figures 4.15-4.19. The measured exhaust emissions at 100% diesel load is represented as a dashed line for comparison. It was expected that

ammonia combustion alone would have produced high amounts of NO due to fuel-bound nitrogen. However, ammonia combustion results in a lower flame temperature that suppresses NO production. These two effects compete with each other and the net results are not straightforward.

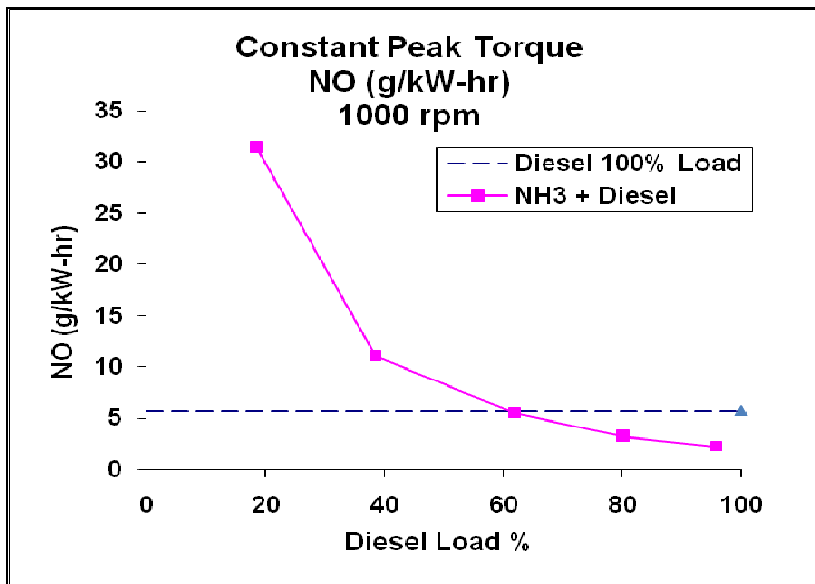


Figure 4.15 - Exhaust NO emissions under constant peak torque operation at 1000 rpm.

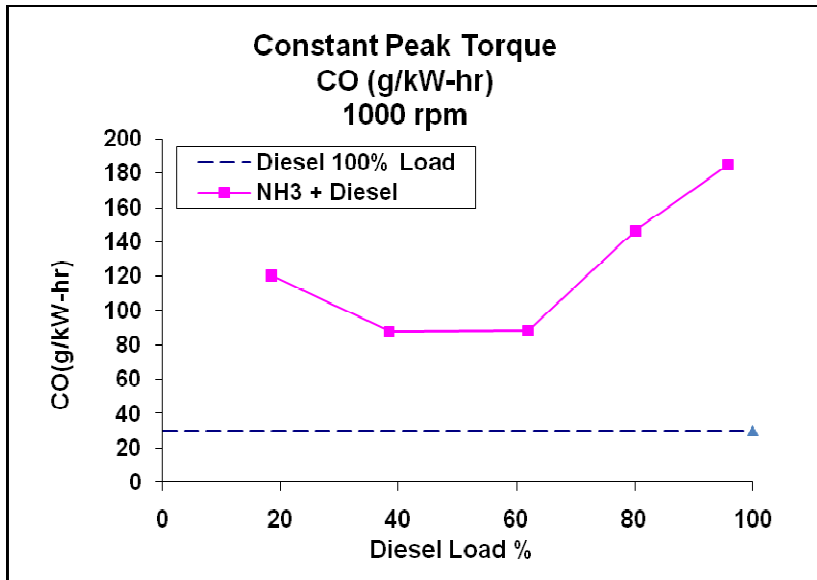


Figure 4.16 – Exhaust CO emissions under constant peak torque operation at 1000 rpm.

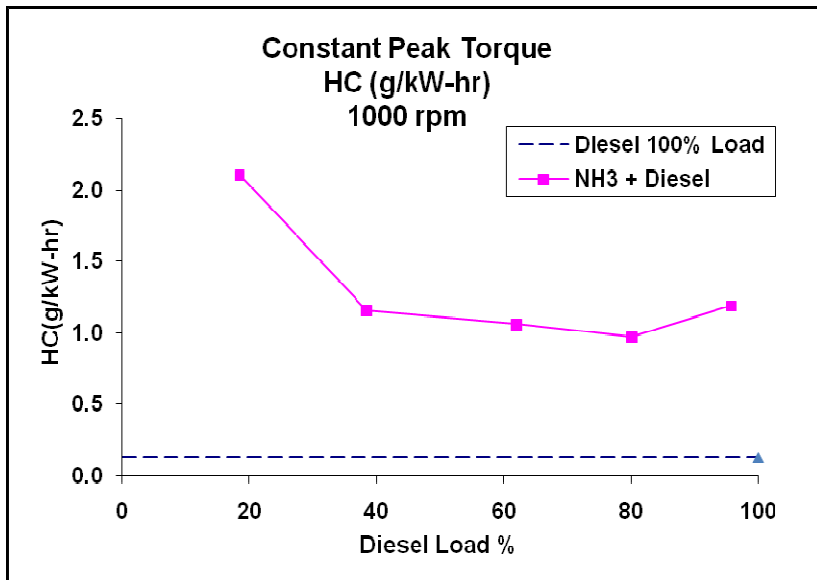


Figure 4.17 – Exhaust HC emissions under constant peak torque operation at 1000 rpm.

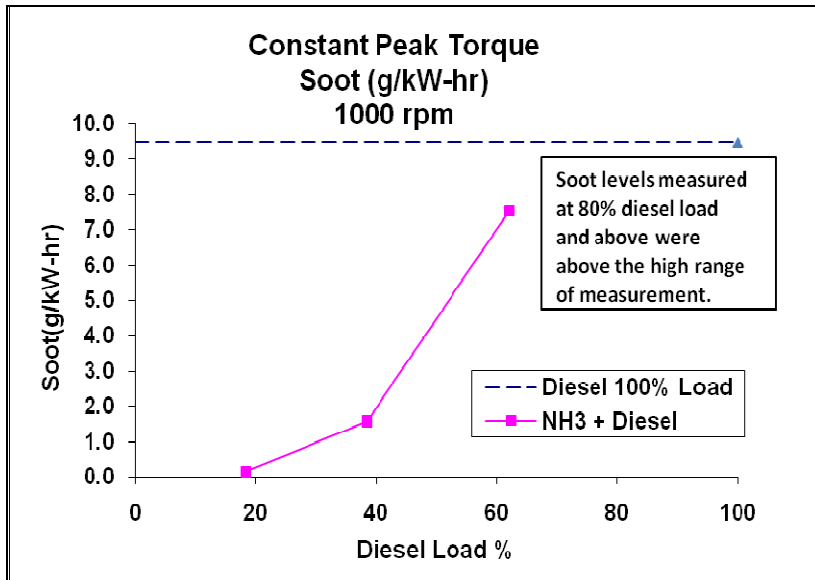


Figure 4.18 – Exhaust soot emissions under constant peak torque operation at 1000 rpm.

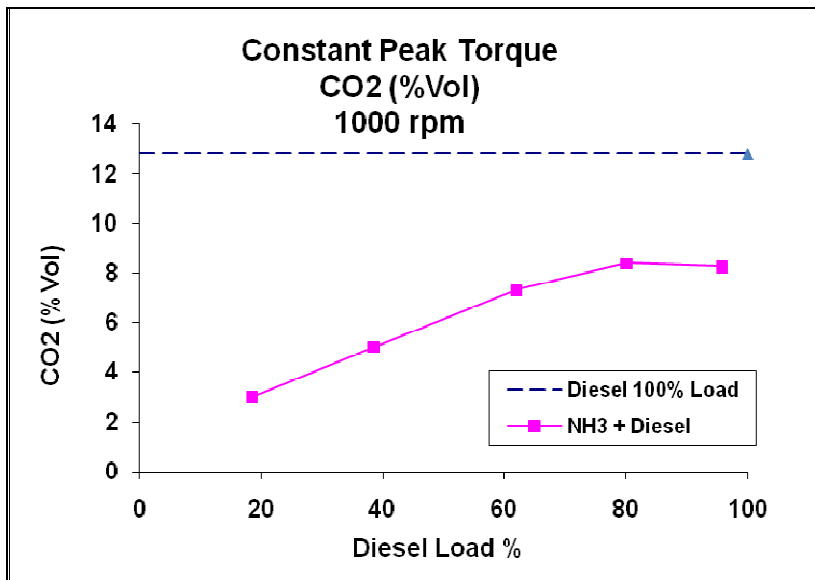


Figure 4.19 – Exhaust CO<sub>2</sub> emissions under constant peak torque operation at 1000 rpm.

It can be seen in Figure 4.15 that when a small amount of diesel fuel is replaced by ammonia (i.e. high diesel load conditions), overall combustion temperature is reduced (Kong and Reiter, 2008) and thus NO emissions are reduced (e.g., 80% and 95% diesel load points).

The effect of fuel-bound nitrogen is less significant in overall NO production. As the amount of ammonia increases (i.e., moving toward lower diesel load points), NO emissions increase. When a significant amount of diesel energy is replaced by ammonia (e.g., 20% diesel load point), NO emissions increase significantly due to the effect of fuel-bound nitrogen. The present emissions results indicate that low NO emissions can be obtained if the diesel load range is higher than 60%. In other words, if the energy substitution of ammonia does not exceed 40% of the total energy, NO emissions will not be a problem.

Figures 4.16 and 4.17 show HC and CO emissions, respectively. It is known that the flame temperature of ammonia is lower than that of diesel fuel (Kong and Reiter, 2008). When ammonia is used to replace part of diesel fuel energy, the overall combustion temperature is lowered. This in turn produces higher HC and CO emissions.

As seen in Figure 4.18, exhaust soot emissions can be reduced if a significant amount of ammonia was used (i.e., diesel fuel energy less than 60%). It is known that soot is produced from the rich zone of diesel combustion. If diesel fuel is reduced significantly, less amounts of diesel fuel will be available for producing soot. On the other hand, soot emissions can be increased if the combustion temperature is reduced due to poor oxidation. At 80% diesel load, there is a significant amount of diesel fuel to produce soot and the combustion temperature is reduced due to ammonia combustion. Therefore, exhaust soot emissions increase significantly.

Figure 4.19 shows that CO<sub>2</sub> emissions decrease significantly as more diesel energy is replaced by ammonia. This effect of ammonia on CO<sub>2</sub> emissions is expected and is one of the main reasons for this study.

Figure 4.20 and 4.21 show exhaust ammonia concentrations measured in ppmV and g/kW-hr under constant peak torque operation. The exhaust ammonia concentrations are well above the OSHA regulatory 50 ppm and the Immediately Dangerous to Life or Health (IDLH) concentration limits of 500 ppm, as seen in Table 4.1. Therefore this dual-fuel combination would not be safely operable without a large supply of fresh air or exhaust after-treatment. The highest concentrations seem to be around the 40% diesel – 60% ammonia operation range.

When normalizing ammonia concentrations by a function of engine power as in Figure 4.21, the engine power used was the total power contributed by both fuels.

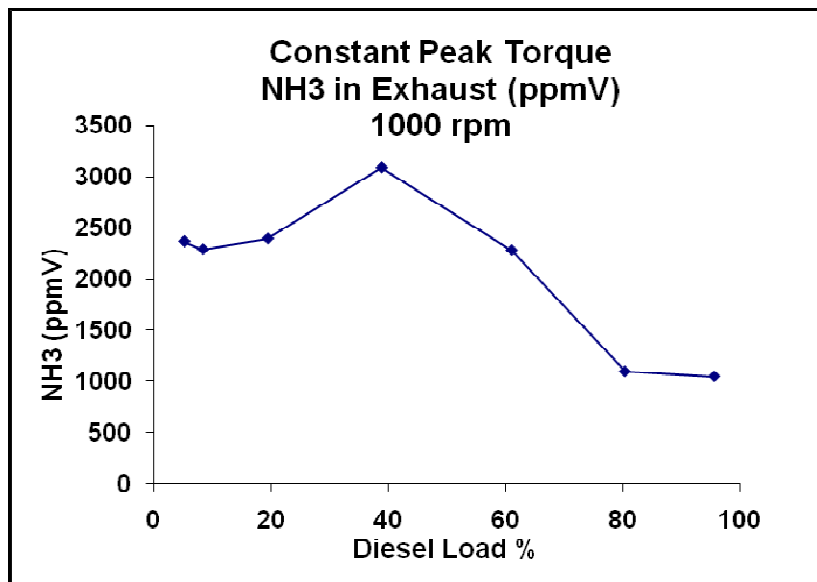


**Figure 4.20 – Exhaust ammonia concentration, ppmV, under constant peak torque operation at 1000 rpm.**

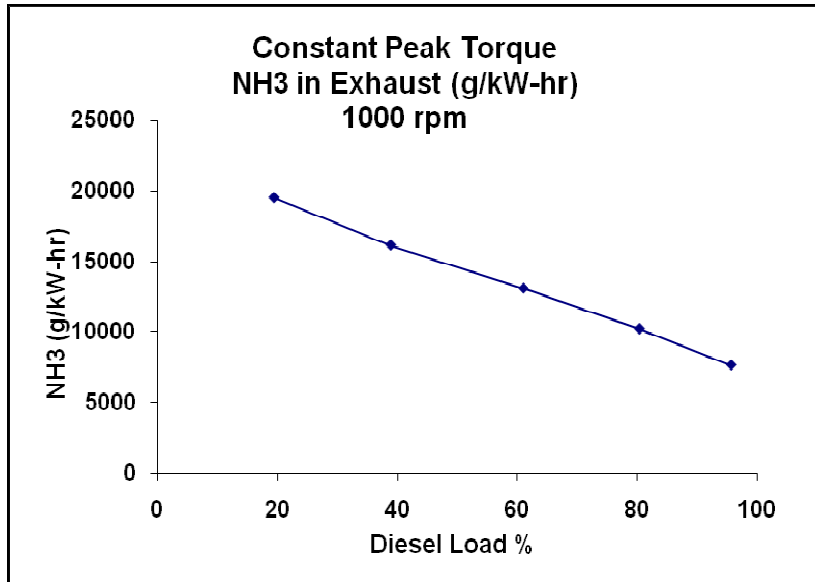


Figure 4.21 – Exhaust ammonia concentration, g/kW-hr, while under constant peak torque operation at 1000 rpm.

**Table 4.1 – Health symptoms due to ammonia exposure (United States Occupational Safety and Health Administration, 2009).**

<b>Ammonia concentration in air (ppm)</b>	<b>Health Symptoms</b>
< 25	Detectable by smell. Maximum Permissible Exposure Limit (PEL) <sup>1)</sup>
30	Uncomfortable, breathing support required. Maximum exposure 15 minutes <sup>1)</sup>
50	OSHA <sup>2)</sup> maximum exposure limit
100	Irritated eyes, throat and mucous membranes. Mild eye, nose, and throat irritation, may develop tolerance in 1-2 weeks with no adverse effects.
140	Moderate eye irritation, no long-term effect in exposures of less than 2 hours
400	Moderate throat irritation. Damage of mucous membranes with more than one hour exposure
500	Immediate danger to life limit (IDLH)
1,000	Caustic to airway
1,700	Fatal after short exposures - less than half an hour
5,000	Immediate hazard to life
> 15,000	Full body protection required
160,000 - 170,000	Flammable in air at 50°C

Combustion efficiency of the ammonia was calculated on volume and mass basis in order to compare methods. The mass flow of ammonia inducted through the intake was a direct measurement. The exhaust ammonia concentration mass flow rate was correlated as described in Eq. (3.5) from the measurements taken using the sample train methodology. Efficiency was then equal to one minus the ammonia exhaust flow divided by the intake flow, in both cases. As can be seen in the results of Figure 4.23, a combustion efficiency range of 91-97% is achievable and both methods provide similar results, although the volume method is generally 1% higher. This shows that although the ammonia may cause disruption of diesel combustion most of it is consumed.

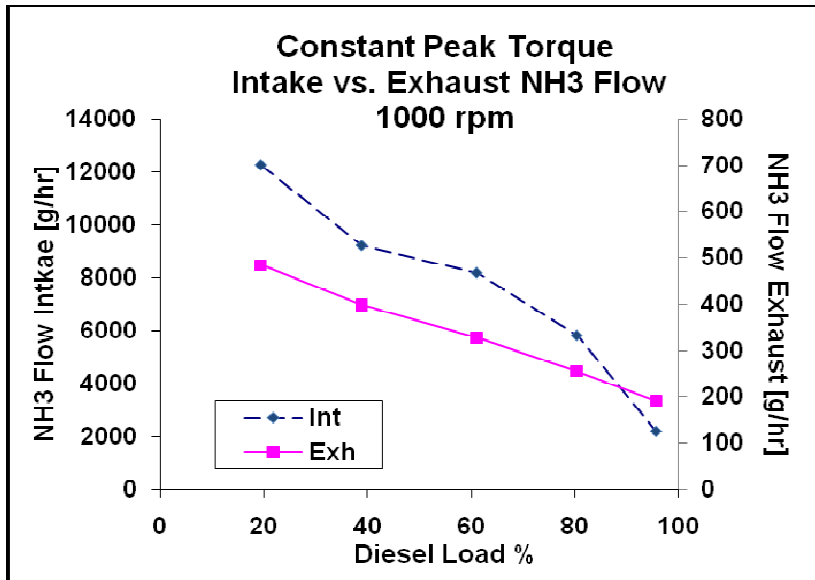


Figure 4.22 – Intake vs. exhaust mass flow of ammonia under constant peak torque operation at 1000 rpm.

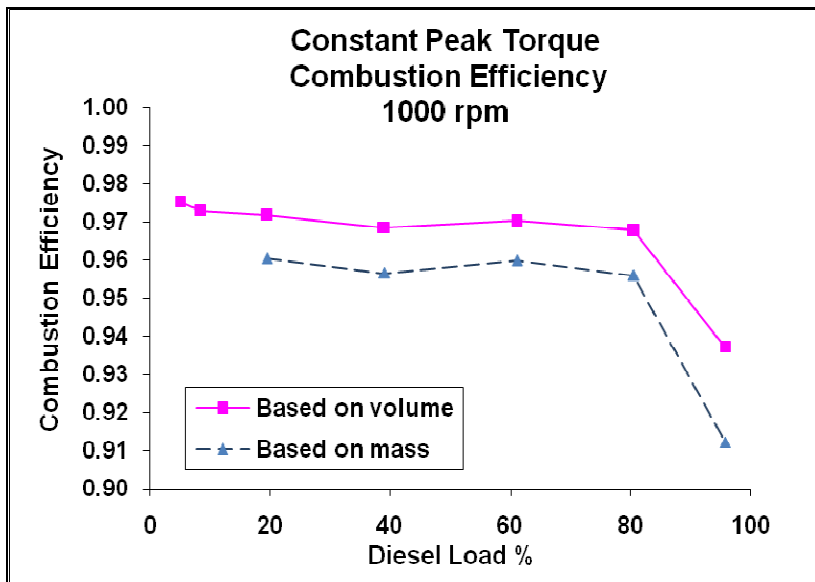


Figure 4.23 – Combustion efficiency of ammonia under constant peak torque operation at 1000 rpm.

Examining the in-cylinder pressure history of 20% diesel plus 80% ammonia, seen in Figure 4.24, it can be seen that large amounts of ammonia result in a long ignition delay. This delay is the main cause in the drop in peak cylinder pressure due to the piston being farther below top-dead-center (TDC). However, combustion duration still occurs in approximately the same amount of time. The premixed burn upon ignition is also more pronounced than the diesel only case.

The heat release rate curve shows that high concentrations of ammonia cause a much later release in energy which agrees with the longer ignition delay. However, the peak of the release is much higher due to the long ignition delay during which more time is available to prepare a combustible mixture.

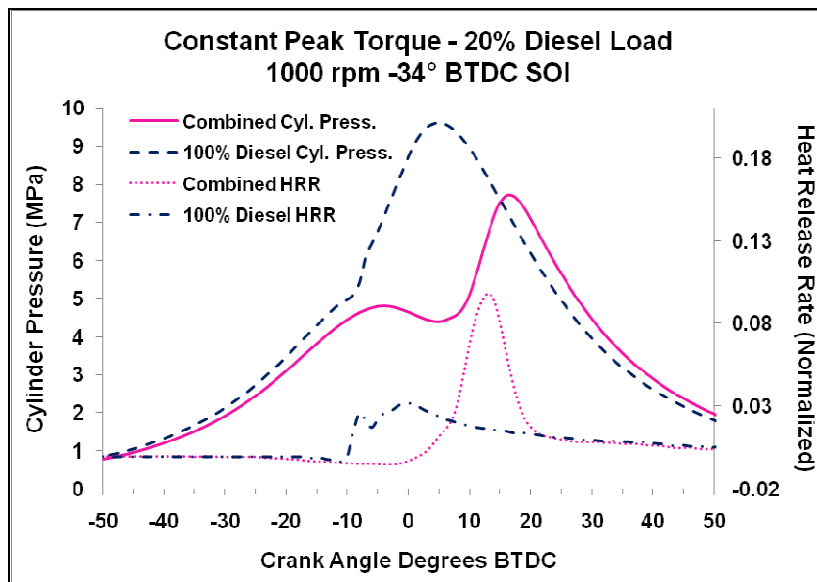


Figure 4.24 – In-cylinder pressure history and heat release rate for 100% diesel fuel and combined diesel-ammonia (20% diesel plus 80%  $\text{NH}_3$ ) under constant peak torque operation.

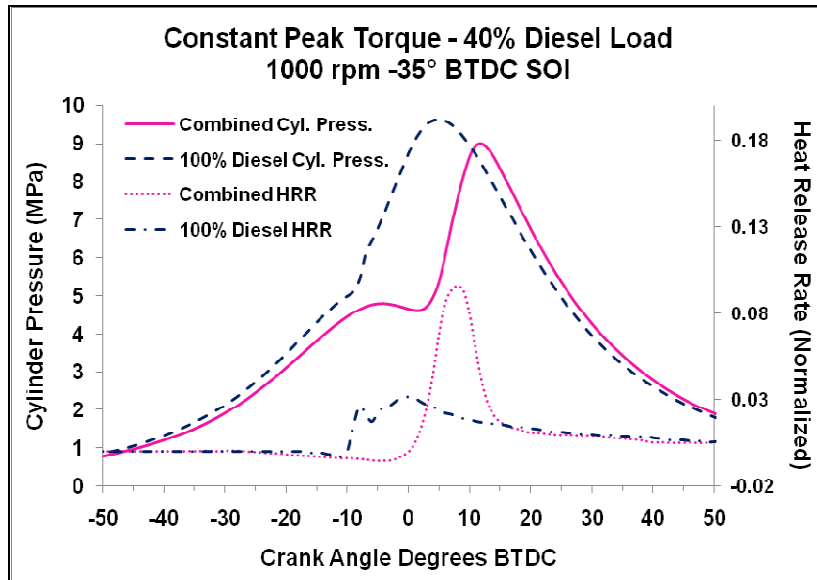


Figure 4.25 – In-cylinder pressure history and heat release rate for 100% diesel fuel and combined diesel-ammonia (40% diesel plus 60%  $\text{NH}_3$ ) under constant peak torque operation.

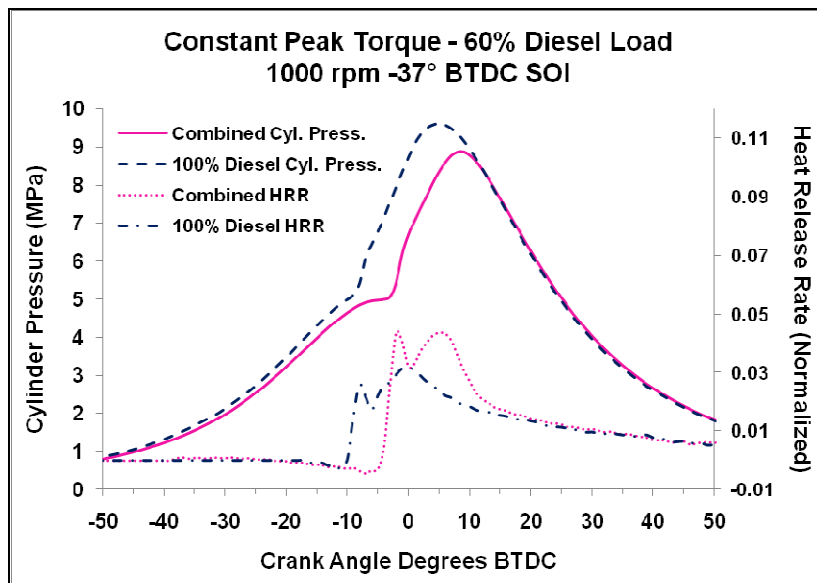


Figure 4.26 – In-cylinder pressure history and heat release rate for 100% diesel fuel and combined diesel-ammonia (60% diesel plus 40%  $\text{NH}_3$ ) under constant peak torque operation.

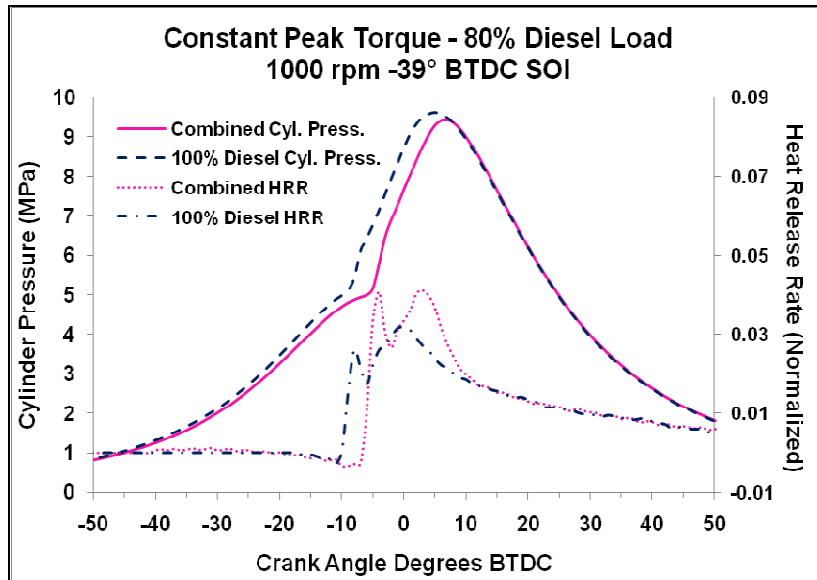


Figure 4.27 – In-cylinder pressure history and heat release rate for 100% diesel fuel and combined diesel-ammonia (80% diesel plus 20%  $\text{NH}_3$ ) under constant peak torque operation.

When comparing pressure traces of the combustion of ammonia and diesel as seen in Figures 4.24-4.27, there seems to be a common trend with increasing the amount of ammonia. There is a longer ignition delay when compared to similar energy representations of 100% diesel loads, and even though engine power output is the same, in-cylinder pressure peaks are reduced until very little ammonia is present, above approximately 80% diesel load.

When examining the heat release rate curves of ammonia combustion, it is seen the start of combustion happens later than diesel fuel alone. This supports the ignition delay observation but its heat release rate has higher peaks.

### 4.2.3 Minimum Diesel Fueling with Variable Ammonia Flow Rates

The next method of engine operation using a dual-fuel approach was to use a minimum amount of diesel fuel and then “throttle” engine load using different ammonia flow

rates. In this testing method, the diesel fuel flow rate was maintained at a level that could produce 5% of diesel only load. Then, the ammonia flow rate was adjusted to control the engine load up to 100%.

Test results are shown in Figures 4.28-4.31. It is indeed feasible to use a small amount of diesel fuel (5% energy) with the maximum amount of ammonia (95% energy) to reach the peak torque conditions. However, the fuel efficiency is relatively low for such conditions. It is thought that the small amount of diesel fuel is not able to provide sufficient ignition energy to the large amount of the ammonia and sustain the rapid flame propagation for ammonia combustion. As a result, BSFC is low. In future studies, a higher diesel fueling rate can be tested to obtain a better efficiency. Notice that the optimal diesel fuel flow rate can depend on the desired engine load.

Due to equipment and facility constraints, testing had to be cancelled without further upgrades. This is why all load points 0-100% are not accounted for in this testing scheme. In future testing this would be completed, but it was felt that enough data had been established to draw the needed conclusions.

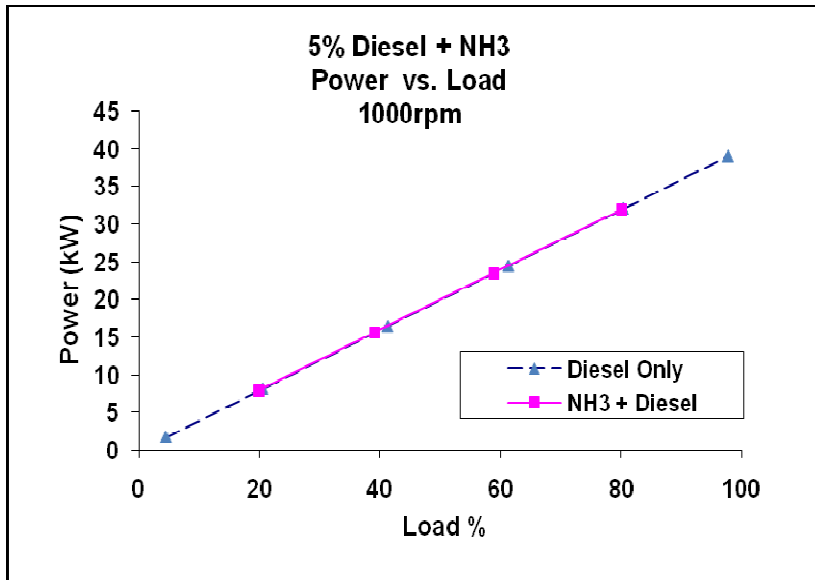


Figure 4.28 – Measured engine power under variable ammonia flow rate operation at 1000 rpm.

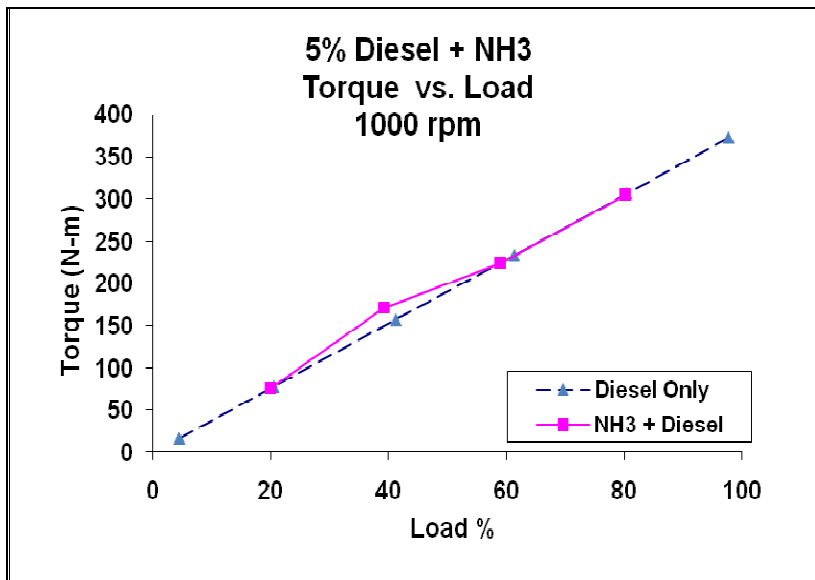


Figure 4.29 – Measured engine torque under variable ammonia flow rate operation at 1000 rpm.

BSFC was calculated based on the respective power contributed by each fuel. In this variable ammonia flow rate operation scheme, diesel fuel flow was held constant and

therefore is represented as a straight line. Since the power contributed by ammonia rises nonlinearly, this causes a downward slope in its BSFC.

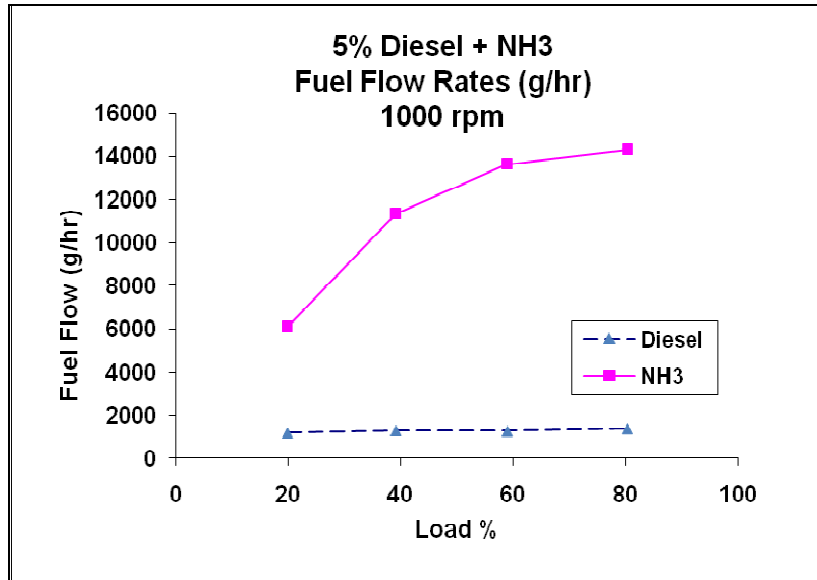


Figure 4.30 – Measured fuel flow rate data under variable ammonia flow rate operation at 1000 rpm.

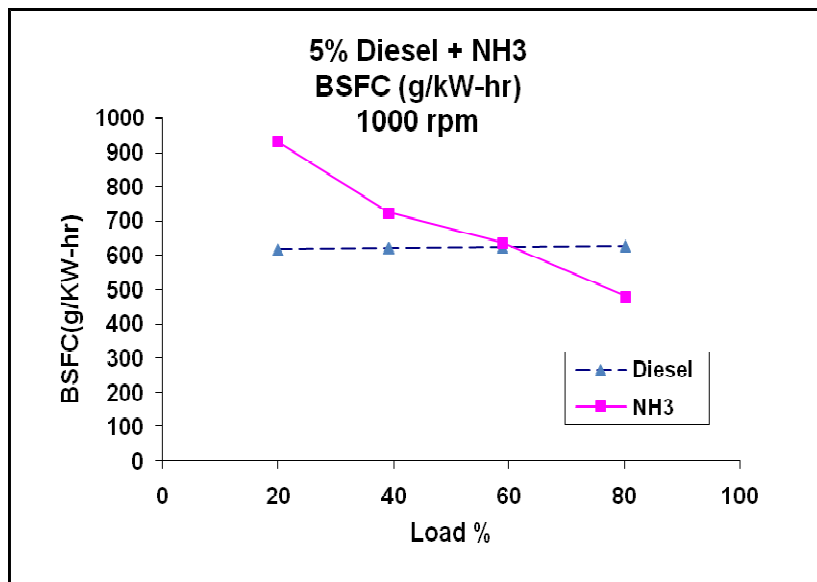


Figure 4.31 – Measured BSFC data under variable ammonia flow rate operation at 1000 rpm.

As can be seen from Figures 4.32 and 4.33, the direct ammonia concentration in the exhaust is significantly higher when the engine is throttled using ammonia as compared to the constant peak torque method earlier.

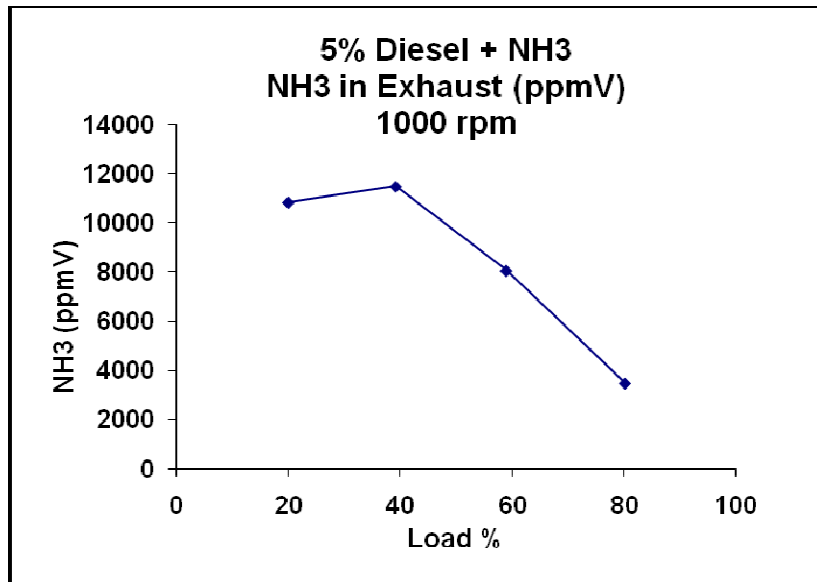


Figure 4.32 – Ammonia concentration in the exhaust, ppmV, under 5% diesel energy with ammonia flow rate operation at 1000 rpm.

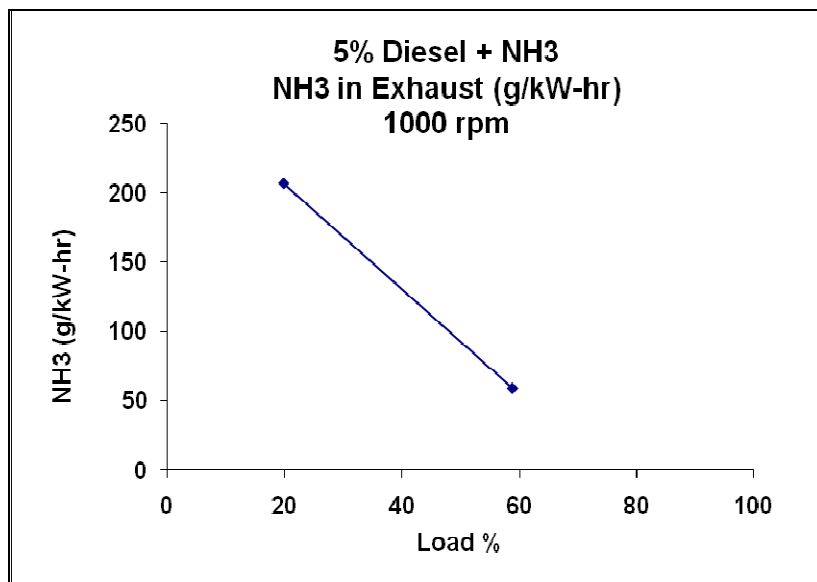
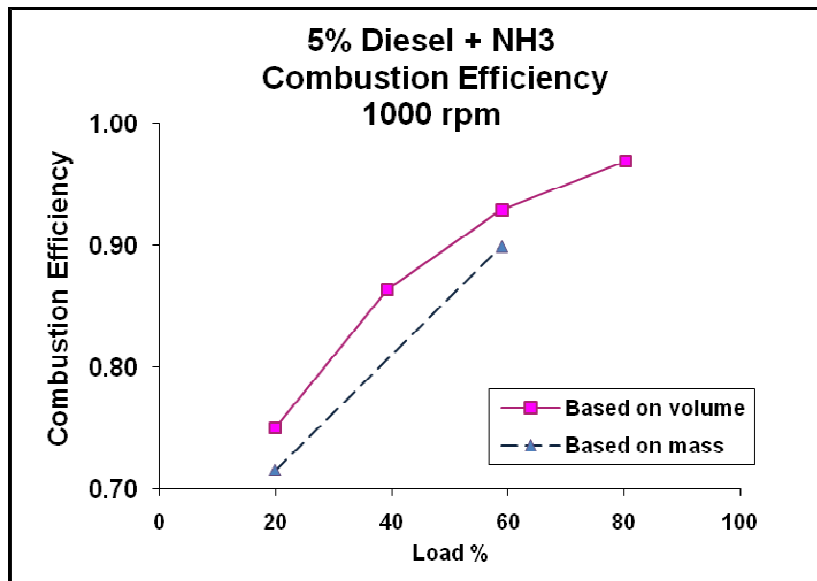


Figure 4.33 – Ammonia concentration in the exhaust, g/kW-hr, under 5% diesel energy with variable ammonia flow rate operation at 1000 rpm.

As can be seen from figure 4.34 the calculated combustion efficiency of this method of operation is lower than that of CPT operation. This is due in part to poor low load efficiency. However, the main cause is due to the small amount of diesel being injected.



**Figure 4.34 – Combustion efficiency of ammonia under 5% diesel energy with variable ammonia flow rate operation at 1000 rpm.**

Figure 4.35 shows the comparison of cylinder pressure histories and heat release rate data using diesel only and combined diesel-ammonia for 20% engine load conditions. In the case of dual-fuel operation, diesel fuel would account for 5% engine load and ammonia would account for 15% load. It can be seen that the dual-fuel operation had a longer ignition delay and lower peak combustion pressure due to long ignition delay caused by ammonia. The overall combustion rate was slower using ammonia since the premixed ammonia-air mixture spread out in the cylinder and required longer combustion duration. On the other

hand, the expansion pressure was slightly lower for the dual-fuel case due to the late combustion of ammonia in the cylinder.

Figure 4.36 shows the results of the 60% engine load condition and similar trends were observed. Since this operating method (5% diesel with variable ammonia) did not produce favorable results due to high fuel consumption and ammonia exhaust emissions, further testing and analyses were not pursued.

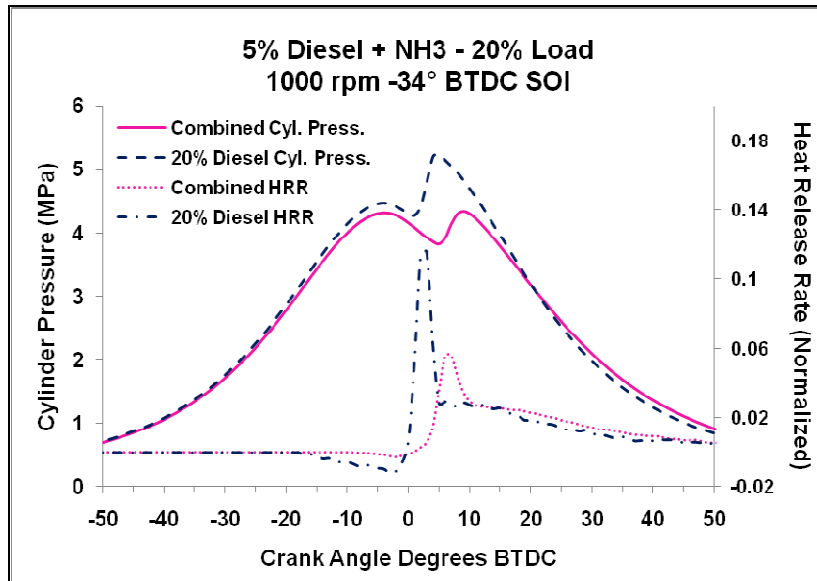


Figure 4.35 – Cylinder pressure histories and heat release rate data for 20% engine load using two different operations at 1000rpm.

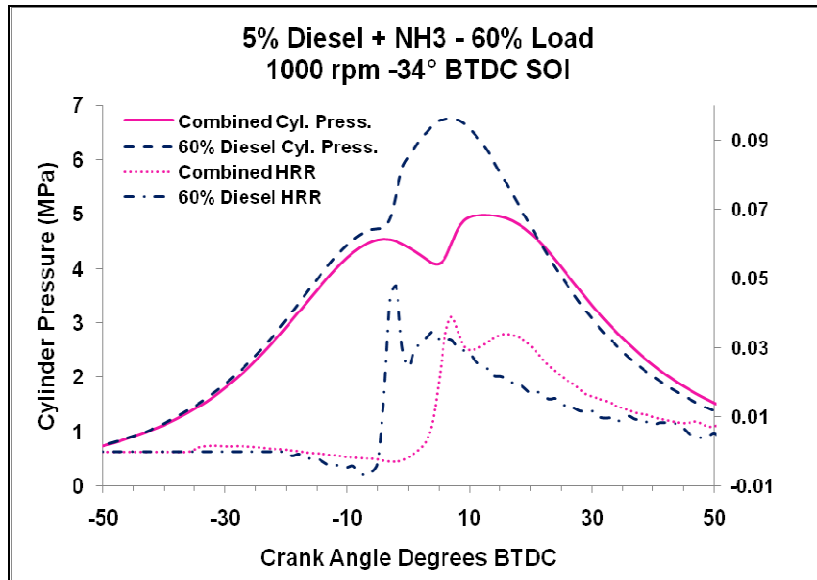


Figure 4.36 – Cylinder pressure histories and heat release rate data for 60% engine load using two different operations at 1000rpm.

#### 4.2.4 Engine Tests Using Biodiesel

Engine tests using pure biodiesel (B100) were also performed. Figures 4.37 and 4.38 show the results of using different combinations of biodiesel and ammonia to maintain a constant peak torque output for 1000 rpm. Furthermore, the engine was operated using 5% biodiesel energy with variable ammonia flow rates to reach desirable engine loads, as shown in Figures 4.39-4.40. Results using biodiesel are similar to those using regular diesel fuel.

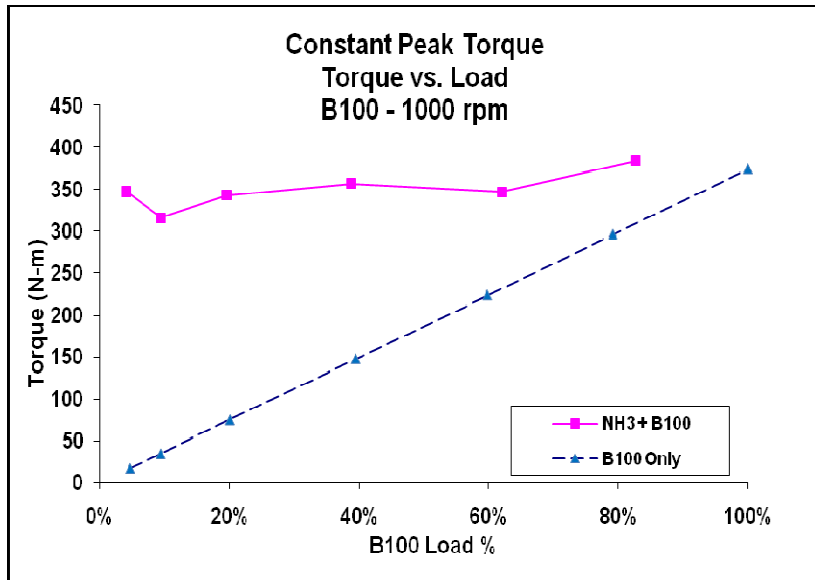


Figure 4.37 – Measured engine torque under constant peak torque operation at 1000 rpm using NH<sub>3</sub> and B100.

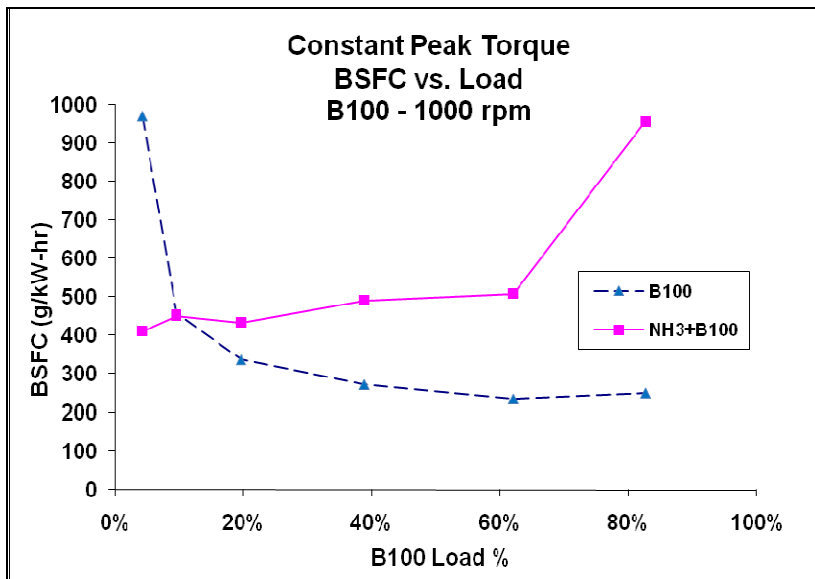


Figure 4.38– Measured BSFC under constant peak torque operation at 1000 rpm using NH<sub>3</sub> and B100.

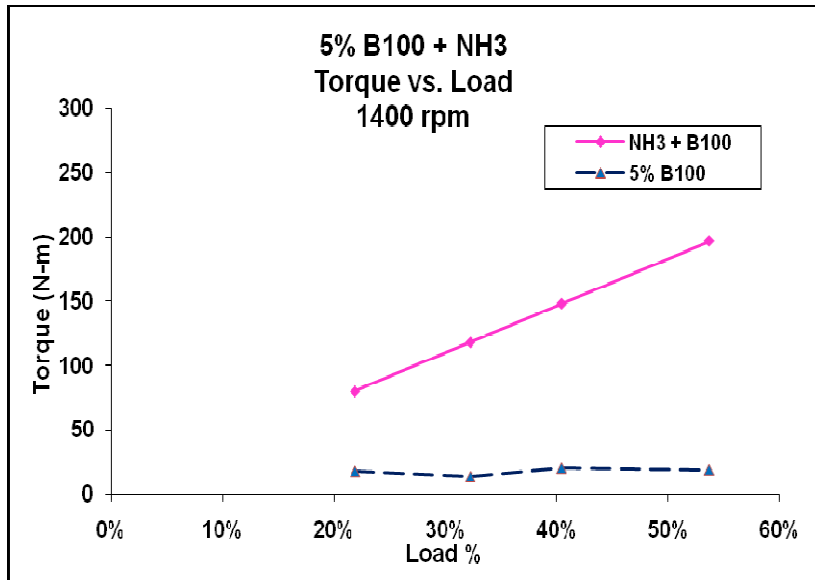


Figure 4.39 – Measured engine torque under variable ammonia flow rate operation at 1400 rpm using NH<sub>3</sub> and B100.

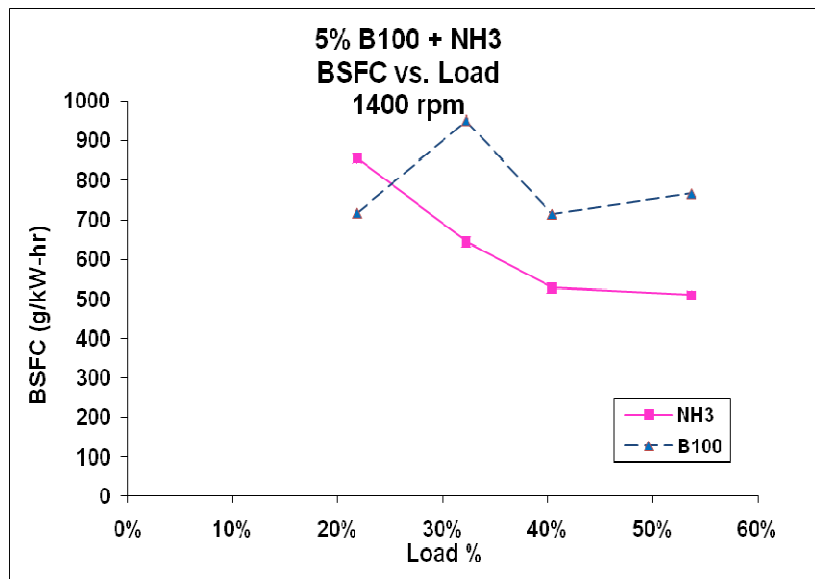
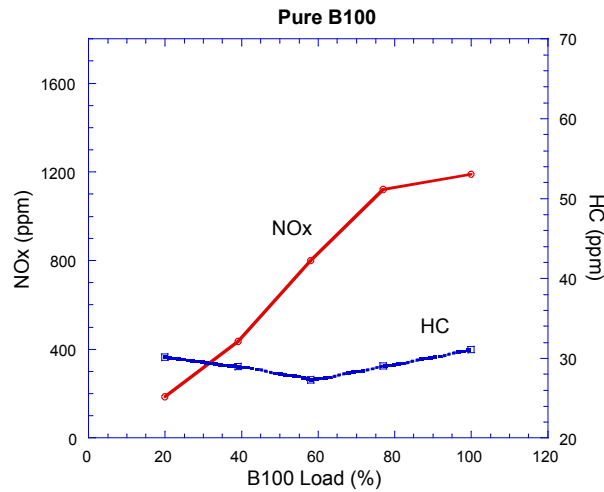
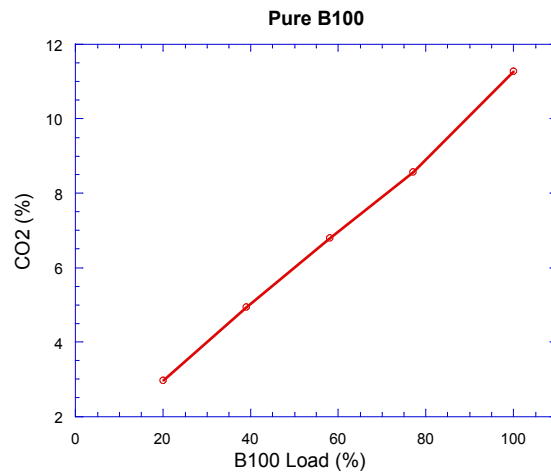


Figure 4.40 – Measured BSFC under variable ammonia flow rate operation at 1400 rpm using NH<sub>3</sub> and B100.

Exhaust emissions using biodiesel and ammonia at various engine load conditions were also measured. Results using B100 only are shown in Figures 4.41-4.42.



**Figure 4.41 – Measured HC and NOx emissions of B100 only.**



**Figure 4.42 – Measured CO<sub>2</sub> emissions of B100 only.**

Figures 4.43-4.45 show NOx, HC, and CO<sub>2</sub> emissions of using pure biodiesel at different engine load conditions using the constant peak torque method, as measured by the DJGAS 5 gas analyzer. The trends are the same as those using regular diesel and ammonia.

In particular, lower NO<sub>x</sub> emissions can be obtained unless a significant amount of biodiesel is replaced by ammonia, e.g., higher than 70% of the total energy.

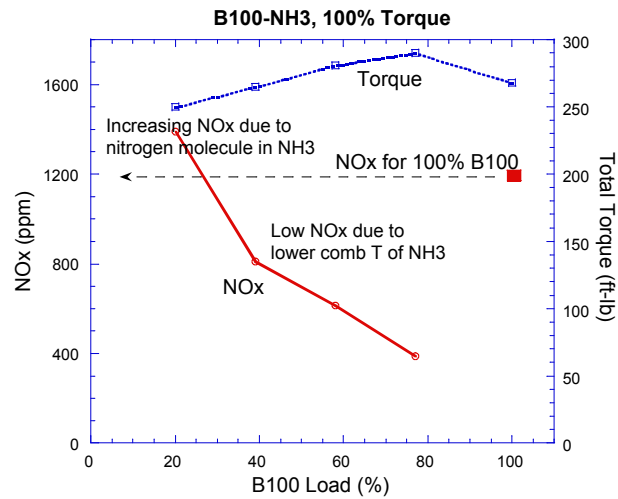


Figure 4.43 – Measured NO<sub>x</sub> emissions of B100 and ammonia under constant peak torque operation.

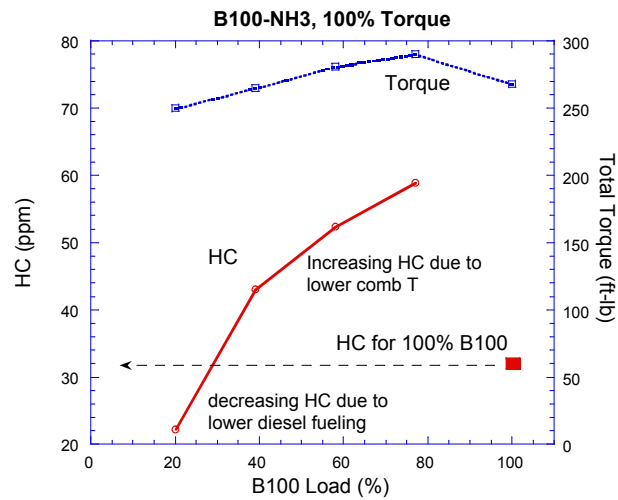


Figure 4.44 – Measured HC emissions of B100 and ammonia under constant peak torque operation.

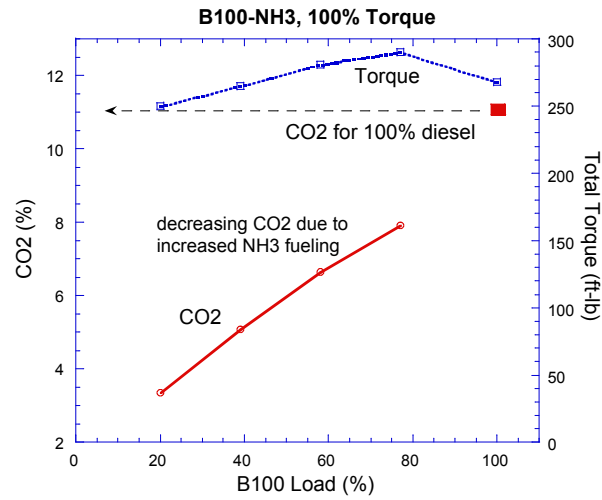


Figure 4.45 – Measured CO<sub>2</sub> emissions of B100 and ammonia under constant peak torque operation.

## 4.2.5 Oil Analysis

Table 4.2 shows the results of engine oil analysis after various testing periods of operation using ammonia. There were concerns on the adverse effects that could be caused by ammonia on the wear metal and lubrication oil. However, as can be seen from Table 4.2, there seems to be little change in oil characteristics over the course of testing with ammonia. Notice that the ASTM limit requires the oil viscosity in the range of 12.5 to 16.3 cSt and the total base number (TBN) higher than 6.

Table 4.2 – Oil sample data as tested by U.S. Oil.

Sample Date	Receipt Date	Brand	Weight	Oil Hrs	Viscosity @ 40C [cSt]	Total Base Number	Water	Solids
5/28/2004	8/22/2008	John Deere	SAE 15-40	5	14.8	11.4	<0.1	0.007
6/4/2004	8/22/2008	John Deere	SAE 15-40	10	14.7	12.2	<0.1	0.007
6/5/2004	8/22/2008	John Deere	SAE 15-40	15	14.7	12.3	<0.1	0.011
6/23/2004	8/22/2008	John Deere	SAE 15-40	20	14.6	11.3	<0.1	0.002
7/14/2004	8/22/2008	John Deere	SAE 15-40	40.5	14.6	11.6	<0.1	0.002

## Chapter 5 Summary and Discussion

### 5.1 Conclusions

This study showed that ammonia could be used as a viable alternative to fossil fuels for compression-ignition. With more research and optimization ammonia could also lead a path to a hydrogen economy through the use of its infrastructure and similar chemistry.

When under constant peak torque operation, as the diesel energy increases beyond 60%, the ammonia-air mixture in the engine may approach its flammability limits and can be too lean to sustain efficient flame propagation for effective combustion. Additionally, the overall combustion temperature is also reduced which in turn deteriorates combustion efficiency. Therefore, the engine brake specific fuel consumption of ammonia is high. On the other hand, when diesel energy is decreased below 40%, the brake specific fuel consumption of diesel fuel is high due to poor part-load efficiency. It appears that from the standpoint of overall fuel efficiency, the favorable operation range using the present dual-fuel approach requires 40~60% diesel energy, i.e., equivalent to 60~40% ammonia energy.

Under constant peak torque operation, if the energy substitution by ammonia is less than 40% (i.e., diesel energy higher than 60%), NO emissions using the dual-fuel operation are lower than using diesel fuel only. This is due to lower thermal NO resulting from the lower combustion temperature involving ammonia. If ammonia energy accounts for more than 60%, exhaust NO emissions increases significantly due to fuel-bound nitrogen in ammonia. On other hand, CO and HC emissions are generally higher for dual-fuel operation when compared to diesel only operation due to the lower combustion temperature of

ammonia. Soot emissions increases for low ammonia fueling but decreases for high ammonia fueling due to the reduced amount of diesel fuel that contributes to soot formation.

The overall combustion efficiency for ammonia is relatively high. However, the exhaust ammonia concentration ranges from 1000-3000 ppmV under constant peak torque operation. Using ammonia to throttle the engine in the variable ammonia flow operation method leads to higher raw levels (ppmV) of  $\text{NH}_3$  in the exhaust.

Analysis of the pressure and heat release data has shown that increasing amounts of ammonia produces a longer ignition delay which results in lower peak combustion pressures as a majority of combustion takes place during piston expansion. On the other hand, the long ignition delay results in a high peaked heat release since the time for mixture preparation has increased and more combustible mixture is available once ignition starts.

## **5.2 Future Study Recommendations**

It was shown the raw ammonia concentrations were not within safe limits. This was also one of the main reasons for halting testing. In order for this to be a viable alternative to fossil fuels other injection/timing methods will have to be tested or an exhaust after-treatment procedure developed.

A better ammonia flow control system can be developed. The author recommends some type of dual needle valve system that has a feedback loop controlled by a computer. The needle valves need to variably adjusted and made of stainless steel or carbon steel with no presence of copper or brass. It is critical that the sealing gaskets be made of Teflon since any rubber will degrade quickly and catastrophically.

Further testing is also recommended in order to optimize combustion. This could involve changing either the pilot fuel and/or the ammonia injection timing. Liquid ammonia delivery could also be investigated in conjunction with direct injection. Both of these techniques are attainable due to increased industry use of electronic and direct injection strategies.

## Bibliography

- Alkemade, U. G., and Schumann, B. (2006). Engines and Exhaust After Treatment Systems for Future Automotive Applications. *Solid State Ionics*, 177(26-32), 2291-2296.
- Bartels, J. (2008). *A Feasibility Study of Implementing an Ammonia Economy*. Iowa State University, Ames, IA.
- Bowman, C. T. (1992). *Control of Combustion-Generated Nitrogen Oxide Emissions: Technology Driven by Regulation*. Paper presented at the Twenty-Fourth Symposium (International) on Combustion The Combustion Institute, Pittsburgh.
- Broadmeadow, J. T., and Ibrahim, O. M. (1995). *Diesel Engine NOx Reduction through Exhaust Re-burning and Ammonia Injection*. Paper presented at the 1995 International Energy Conversion Engineering Conference.
- Caton, J. A., and Siebers, D. L. (1989). Comparison of Nitric Oxide Removal by Cyanuric Acid and by Ammonia. *Combustion Science Technology* 65, 277-293.
- Caton, J. A., and Xia, Z. (2004). The Selective Non-Catalytic Removal (SNCR) of Nitric Oxides from Engine Exhaust Streams: Comparison of Three Processes. *Journal of Engineering for Gas Turbines and Power*, 126.
- Central Intelligence Agency (Producer). (2009, March 21, 2009) The World Factbook. <https://www.cia.gov/library/publications/the-world-factbook/print/xx.html>.
- Energy Information Administration (1998). Alternatives to Traditional Transportation Fuels 1998. *DOE/EIA-0585(98)*.

Environmental Defense Fund (Producer). (2002, March 21, 2009) NOx Fact Sheet.

[http://www.edf.org/documents/2551\\_FactSheet\\_NOx.pdf](http://www.edf.org/documents/2551_FactSheet_NOx.pdf).

Environmental Protection Agency (1997). Procedure for Collection and Analysis of

Ammonia in Stationary Sources (CTM-027). Washington: GPO.

Gieshoff, J., Pfeifer, M., Schafer-Sindlinger, A., Spurk, P., Garr, G., and Leprince, T. (2001).

Advanced Urea SCR Catalysts for Automotive Applications. *SAE Technical Papers 2001-01-0514*.

Gray, J. T., Dimitroff, E., Meckel, N. T., and Quillian, R. D. J. (1966). Ammonia Fuel --

Engine Compatibility and Combustion. *SAE Technical Papers 660156*.

Hui, H., Clarke, R., and Burns, S. (Producer). (2008, Dec.19, 2008) Ammonia Prices and

Pricing Information.

<http://www.icis.com/v2/chemicals/9075153/ammonia/pricing.html>

ICIS (Producer). (2007, Dec. 19, 2008) Ammonia Uses and Market Data.

<http://www.icis.com/v2/chemicals/9075154/ammonia/uses.html>.

Javed, T. M., Irfan, N., and Gebbs, B. M. (2007). Control of Combustion-Generated Nitrogen

Oxides by Selective Non-Catalytic Reduction. *Journal of Environmental Management*, 83, 251-289.

Kimball-Linne, M. A., and Hanson, R. K. (1986). Combustion-Driven Flow Reactor Studies

of Thermal DeNOx Reaction Kinetics. *Combustion and Flame*, 64, 337-351.

Koch, E. (1945). Ammonia - A Fuel for Motor Buses. *J. Inst. Pet.* , 31, 213.

- Kong, S. C., and Reiter, A. (2008). Demonstration of Compression-Ignition Engine Combustion using Ammonia in Reducing Greenhouse Gas Emissions. *Energy and Fuels*, 22, 2963-2971.
- Lambert, C., Cavataio, G., Cheng, Y., Dobson, D., Girard, J., Laing, P., Patterson, J., and Williams, S. (2006). Urea SCR and DPF System for Tier 2 Diesel Light-Duty Trucks. Unpublished Presentation. Ford Research and Advanced Engineering.
- MacKenzie, J., and Avery, W. (1996). Ammonia Fuel: The Key to Hydrogen-Based Transportation. *IEEE Technical Papers 96556*.
- Miller, J. A. (1996). *Theory and Modeling in Combustion Chemistry*. Paper presented at the Twenty-Sixth Symposium (International) on Combustion The Combustion Institute, Pittsburgh.
- Miyamoto, N., Ogawa, H., Wang, J., Shudo, T., and Yamazaki, K. (1995). Diesel NO<sub>x</sub> Reduction with Ammonium Deoxidizing Agents Directly Injected into the Cylinder. *International Journal of Vehicle Design*, 16(1), 71-79.
- Modak, J. M. (2002). Haber Process for Ammonia Synthesis. *Resonance*, 69-77.
- Muzio, L. J., Martz, T. D., Montgomery, T. A., Quartucy, G. C., Cole, J. A., and Kramlich, J. C. (1990, Nov). *N<sub>2</sub>O Formation in Selective Non-Catalytic Nitric Oxides Reduction Process*. Paper presented at the Fall International Symposium of the American Flame Research Committee, San Francisco.
- National Institute of Standards and Technology (2009). NIST Webbook Retrieved January, 2009

- Pearsall, T., and Garabedian, C. (1967). Combustion of Anhydrous Ammonia in Diesel Engines. *SAE Technical Papers 670947*.
- Saika, T., Nakamura, M., Nohara, T., and Ishimatsu, S. (2006). Study of Hydrogen Supply System with Ammonia Fuel. *JSME International Journal*, 49(1), 78-83.
- Sato, T., Hamada, A., and Kitamura, K. (1998). A Feasibility Study of Conceptual Design for International Clean Energy Network Using Hydrogen Conversion Technology *WE-NET Annual Reports*.
- Shah, S. D., Mauti, A., Richert, J., Loos, M., and Chase, R. (2007). Measuring NO<sub>x</sub> in the Presence of Ammonia. *SAE Technical Papers 2007-01-0331*.
- Starkman, E. S., Newhall, H. K., Sutton, R., Maguire, T., and Farbar, L. (1966). Ammonia as a Spark Ignition Engine Fuel -- Theory and Application. *SAE Technical Papers 660155*.
- Ullmann's Encyclopedia of Industrial Chemistry (Ed.) (2006) Ullmann's Encyclopedia of Industrial Chemistry. Weinheim: Wiley-VCH.
- United States Occupational Safety and Health Administration (Producer). (2009, March 21, 2009) Safety and Health Topics: Ammonia.  
[http://www.osha.gov/dts/chemicalsampling/data/CH\\_218300.html](http://www.osha.gov/dts/chemicalsampling/data/CH_218300.html).
- Williams, J. L. (Producer). (2009, March 21, 2009) Oil Price History and Analysis.  
<http://www.wtrg.com/prices.htm>.
- Xu, L., McCabe, R., and Hammerle, R. (2002). NO<sub>x</sub> Self-Inhibition in Selective Catalytic Reduction with Urea (Ammonia) Over a Cu-Zeolite Catalyst in Diesel Exhaust. *Applied Catalysis B: Environmental*, 39(1), 51-63.